NOVEMBER 2025 M.Sc. in Industrial Engineering LANA MANLA ALI

REPUBLIC OF TÜRKİYE

GAZIANTEP UNIVERSITY

GRADUATE SCHOOL OF NATURAL & APPLIED SCIENCES

A PATH-DEPENDENT MULTI-PERIOD REBALANCING MODEL FOR STOCHASTIC U-SHAPED DISASSEMBLY LINES

M.Sc. THESIS

IN

INDUSTRIAL ENGINEERING

BY

LANA MANLA ALI

NOVEMBER 2025

A PATH-DEPENDENT MULTI-PERIOD REBALANCING MODEL FOR STOCHASTIC U-SHAPED DISASSEMBLY LINES

M.Sc. Thesis

in

Industrial Engineering

Gaziantep University

Supervisor

Prof. Dr. Eren ÖZCEYLAN

Co-Supervisor

Assoc. Prof. Dr. Süleyman METE

by

Lana MANLA ALI

November 2025

I hereby declare that all information in this document has been obtained and presented in accordance with academic rules and ethical conduct. I also declare that, as required by these rules and conduct, I have fully cited and referenced all material and results that are not original to this work.

Lana MANLA ALI

ABSTRACT

A PATH-DEPENDENT MULTI-PERIOD REBALANCING MODEL FOR STOCHASTIC U-SHAPED DISASSEMBLY LINES

MANLA ALI, Lana
M.Sc. in Industrial Engineering
Supervisor: Prof. Dr. Eren ÖZCEYLAN
Co-Supervisor: Assoc. Prof. Dr. Süleyman METE
November 2025
72 pages

With the increasing environmental concerns and stricter regulations, manufacturers face serious pressure to design sustainable and efficient end-of-life (EoL) product recovery systems. Disassembly plays a central role in these systems, yet keeping disassembly lines balanced and efficient under the changing conditions of real-world remains a major challenge. In practice, these conditions often require rebalancing the line. Unlike existing studies that consider rebalancing as a one-time independent adjustment, this study proposes a Mixed-Integer Linear Programming (MILP) model for multi-period, path-dependent rebalancing of U-shaped disassembly lines reflecting the sequential nature of real operations where each decision shapes the next. To address uncertainty, a chance constraint is incorporated for stochastic task times, while the objective minimizes both task relocation and workstation operating costs as demand vary. Tested and benchmarked on different instances, the findings showed that the proposed model achieved cost savings of approximately 20% under high-demand conditions, 17% under cyclical demand, and 5% under low-demand scenarios outperforming the independent rebalancing strategy commonly adopted in the literature. To the best of our knowledge, this is the first study integrating U-shaped layouts, stochastic task times, and path-dependent rebalancing, providing a flexible decision-support tool for managers in dynamic environments.

Key Words: Disassembly Line, Rebalancing, Path-dependent, U-shaped, MILP, Multi-period

ÖZET

STOKASTİK U-TİPİ DEMONTAJ HATLARI İÇİN YOL BAĞIMLI ÇOK PERİYOTLU YENİDEN DENGELEME MODELİ

MANLA ALI, Lana
Yüksek Lisans Tezi, Endüstri Mühendisliği Bölümü
Danışman: Prof. Dr. Eren ÖZCEYLAN
İkinci Danışman: Assoc. Prof. Dr. Süleyman METE
Kasım 2025
72 sayfa

Artan çevresel kaygılar ve sıkılaşan düzenlemeler, üreticileri sürdürülebilir ve verimli ürün yaşam sonu (EoL) geri kazanım sistemleri tasarlamaya zorlamaktadır. Bu sistemlerde, demontaj, merkezi bir rol oynamaktadır. Ancak, gerçek dünyadaki değişen koşullar altında, demontaj hatlarını dengede ve verimli tutmak, büyük bir zorluk olmaya devam etmektedir. Bu koşullar, hattın yeniden dengelenmesini gerektirir. Mevcut çalışmalardan farklı olarak, bu çalışma, yeniden dengelemeyi tek seferlik bağımsız bir ayarlama olarak değil, her kararın bir sonrakini şekillendirdiği, operasyonların sıralı doğasını yansıtacak şekilde ele almaktadır. Bu amaçla, U şeklindeki demontaj hatlarının çok dönemli, yol bağımlı yeniden dengelenmesi için karışık tamsayılı doğrusal programlama (MILP) modeli önerilmektedir. Belirsizlik için, stokastik görev sürelerine yönelik bir şans kısıtı eklenmiştir. Amaç fonkisyonu, talebin değişmesine bağlı olarak görev yeniden yerleştirme ve iş istasyonu işletme maliyetlerini en aza indirmektir. Test sonuçları, modelin yüksek talepte %20, döngüsel talepte %17 ve düşük talepte %5 maliyet tasarrufu sağladığını göstermektedir. Ayrıca literatürde yaygın olan bağımsız yeniden dengeleme stratejisini geride bırakmaktadır. Bu çalışma, U-tipi hatları, stokastik görev sürelerini ve yol-bağımlı yeniden dengelemeyi entegre eden ilk çalışmadır. Dinamik ortamlarda yöneticiler için esnek bir karar destek aracı sunmaktadır.

Anahtar Kelimeler: Demontaj hattı, Yeniden dengeleme, Yola bağlılık, U-tipi, MILP, Çok periyotlu

''Dedicated to my family and to Lilla Alina'

- Lana Manla ali

ACKNOWLEDGEMENTS

First and foremost, I would like to express my heartfelt gratitude to my supervisor, Prof. Dr. Eren ÖZCEYLAN, and my co-supervisor, Assoc. Prof. Dr. Süleyman METE, for their invaluable guidance, insightful feedback, and support throughout the course of this study. I am truly grateful for their patience, their mentorship, and for always being generous with their time, wisdom, and trust in my capabilities.

I extend my deepest appreciation to my family, whose unconditional love and unwavering support have carried me through every challenge. Their faith in me has been the foundation of my strength. Thank you for standing by me with open hearts and open arms, for your prayers, and for always holding space for me to grow.

To my dearest friends, thank you for being my escape, my laughter, and my comfort. Your kind words and uplifting presence made the difficult days bearable and the joyful moments even more meaningful. I am deeply grateful for your constant support and for always seeing the best in me.

I am especially grateful to the loved ones…, those who stood by me without needing explanations, and to whom who believed in me the most. Among all the voices that reached out, there was one whose words always carried more weight, whose faith in me was a lifeline. A single word of encouragement from them could silence all my doubts, could remind me of my strength, and made me want to become someone they would never be disappointed in. Their quiet support was not just comforting; it was transformative. And though they may never know the depth of their impact, I carry it with me always, like a light that never fades.

TABLE OF CONTENTS

LIST OF TABLES

Page

LIST OF FIGURES

Page

CHAPTER 1
INTRODUCTION

1.1 Motivation of Study

In recent years, with the increasing environmental concerns and stricter government regulations, manufacturers face serious pressure to design sustainable and efficient end-of-life (EoL) product recovery systems. Among various recovery strategies, the reuse of EoL products plays an important role in reducing both environmental pollution and manufacturing costs (Farahani et al. 2019). For that, the disassembly process, constitute a critical phase in the product recovery process, which enables the extraction of reusable components out of a certain product and that consequently help reduce the environmental waste. The disassembly process is particularly important in sectors such as electronics, appliances, and automotive industries, where the products may contain hazardous and high-value materials and the product is disassembled in order to reuse such components. Consequently, the organization and operational efficiency of disassembly systems have become a key concern for manufacturers, researchers, and policymakers alike.

Despite its importance, the disassembly process introduces a range of operational challenges. Unlike the assembly process, which is typically more standardized and deterministic in its nature, disassembly must deal with considerable uncertainty and variability. The returned products may differ significantly in design, condition, and composition. Some components may be missing, damaged, or unsuitable for recovery, and that directly affects disassembly times and task feasibility. Furthermore, the sequence in which disassembly tasks can be performed is governed by what called precedence constraints, which are often more complex than the ones in the assembly operations due to potential *AND/OR* relations and conditional dependencies.

Among the operational challenges in disassembly systems, line balancing plays a central role. The Disassembly Line Balancing Problem (DLBP) involves assigning disassembly tasks to workstations in such a way that optimizes a one or more performance criteria, such as minimizing the number of stations, reducing idle time, or minimizing cycle time while adhering to precedence relations and task times constraints (Güngör and Gupta 1999). Thus, achieving an efficient balance directly impacts the overall performance of the disassembly process, influencing throughput, resource utilization, and environmental outcomes.

The DLBP is inherently considered more complex than traditional assembly line balancing problem (ALBP). This complexity is due to factors like reverse material flows, where instead of building a product from components, disassembly systems decompose products into their constituent parts. In addition, the condition of returned EoL products is rarely consistent, there could be many variations in wear, contamination, or damage of a product affect operation time leading to increased uncertainty in task times (Özceylan et al. 2018). Therefore, designing and balancing disassembly lines effectively is not only key to enhancing operational efficiency but also critical for meeting broader environmental objectives (Güngör and Gupta 2002).

In dynamic production environments, disassembly systems frequently encounter disruptions that are driven by factors such as fluctuating demand of the recovered components, frequent changes in product design, and the unpredictable quality and mix of returned products. Such disruptions impose considerable challenges on maintaining a balanced and efficient disassembly line, often necessitating re-balancing efforts to adapt the system layout and task assignments to the current operational changes. As a result, rebalancing becomes a crucial strategy to maintain effective operations under changing conditions. In the context of disassembly systems, rebalancing refers to the process of modifying an existing task-to-station assignment in a previously balanced line in response to changes in operational conditions. It is a corrective strategy employed to restore or enhance the performance of a line that has become inefficient or infeasible due to new constraints, variations in product mix, fluctuations in demand, changes in task times, or modifications in system layout. It involves reassigning tasks to different stations, adjusting workstation loads, or even changing the number of stations to restore or improve performance. While several studies have explored line rebalancing as a one-time process, these typically mean that the system is re-optimized from the initial configuration repeatedly whenever a disruption or change occurs.

This approach treats each rebalancing event as independent, assuming that the system can be reset to its original state without considering the impact of prior adjustments. Although this simplification facilitates model formulation and computational analysis, it significantly deviates from real-world disassembly operations, where system configurations evolve over time and are shaped by the cumulative effects of past decisions. In contrast, real-world disassembly systems evolve, (i.e., previous configurations influence future decisions) once a disassembly line is rebalanced, its new configuration becomes the operational baseline for subsequent adjustments, thus, rebalancing is not isolated but rather sequential and path-dependent with each decision shaping the next. This highlights the need for a sequential rebalancing framework observed over multiple periods, where rebalancing decisions are considered in a path-dependent manner. The concept of path-dependency refers to situations where past decisions, events, or states influence the present and future possibilities, often limiting or guiding the choices that can be made over time. Thus, such a framework acknowledges that the configuration of a disassembly line disassembly line in a given period directly influences the starting point for the next, thereby introducing a temporal dependency across planning horizons, supporting progressive optimization, where the line continuously learns and adapts through a series of interconnected adjustments rather than through repetitive resets to an initial state. This approach enhances the system's resilience, reduces unnecessary reconfiguration costs, and aligns the decision-making process more closely with the long-term operational objectives of sustainable and flexible disassembly systems.

Another critical aspect to be considered is the design of the disassembly line layout, which significantly affects the system's adaptability and performance. Among many layout types, the U-shaped line layout has gained a lot of attention due to its significant advantageous such as its inherent flexibility and ergonomic efficiency. U-shaped lines are characterized by a layout in which the entrance and exit points are located at the same end of the line, allowing tasks to be performed from both the front and back sides of the line which enhances flexibility, reduces walking distances, and promotes worker collaboration, especially in environments with high product variability. While U-shaped layouts have been extensively studied in assembly line contexts, including stochastic scenarios (Delice et al. 2016), their application in disassembly line rebalancing domain remains unexplored, as no prior study in the literature ever considered studying the rebalancing of disassembly lines on U-shaped layouts. This highlights a significant research gap and an opportunity to extend the benefits of U-shaped layouts to the disassembly line rebalancing literature.

To address the aforementioned challenges and bridge the identified research gaps, this thesis proposes a novel stochastic, multi-period sequential rebalancing model for U-shaped disassembly lines. The proposed model is designed to capture the dynamic, uncertain, and evolving nature of real-world disassembly operations while promoting efficiency, flexibility, and stability over time. The model incorporates the following key innovations:

- Sequential rebalancing framework: Unlike one-time rebalancing approaches, the proposed model introduces a path-dependent structure where each period's solution is influenced by the prior configuration.
- U-shaped layout adaptation: The model explicitly considers U-shaped line configurations, enabling bidirectional task assignments and enhancing layout flexibility.
- Stochastic task times: To capture real-life variability in task durations, the model employs chance-constrained approach, ensuring that task assignments remain feasible under uncertainty.
- Demand-driven cycle time variation: The model operates under scenarios where customer demand changes across periods, necessitating adjustments in the cycle time to accommodate demand fluctuations.
- Rebalancing cost minimization: The model incorporates rebalancing cost components to penalize task reassignment and promote stability across periods.

To the best of our knowledge, this is the first study that combines stochastic task times, U-shaped line structures, and sequential rebalancing in the line rebalancing literature, specifically, the disassembly domain.

The remainder of this thesis is structured as follows: Chapter 2 presents a review of the relevant literature on assembly and disassembly line rebalancing.

Chapter 3 defines the problem and details the formulation of the proposed mathematical model. In Chapter 4, The methodology and an illustrative example is introduced to demonstrate and validate the model. Chapter 5 discusses the experimental design established for this study, along with the computational results obtained from applying the developed model and a comparative analysis to evaluate the effectiveness of the proposed approach.

Finally, Chapter 6 concludes the thesis by summarizing the main findings, discussing the practical implications, and proposing directions for future research.

CHAPTER 2
LITERATURE REVIEW

Assembly and disassembly line balancing problems (ALBPs and DLBPs) have been widely studied in the literature due to their practical importance in optimizing manufacturing and remanufacturing systems. A significant portion of this body of research has focused on rebalancing, which becomes essential in response to various dynamic changes such as product redesigns, demand shifts, workforce changes, or disruptions like task failures.

The rebalancing of assembly lines has been studied extensively in the literature, with various models and solution techniques proposed. Contributions include the works of (Gamberini et al., 2006, 2009; Agpak, 2010; Yang et al., 2013; Zha and Yu, 2014; Celik et al., 2014) who approached the problem through heuristic and metaheuristic methods. In parallel, exact approaches were developed to evaluate conditions under which rebalancing is economically justified. Corominas et al. (2008) proposed a binary mathematical model aims to minimize the number of temporary workers in response to fluctuating demand. Subsequent works introduced cost-focused mathematical formulations. Altemeier et al. (2009) presented a model minimizing costs from overload and workforce rearrangements. Similarly, Oliveira et al. (2012) tackled mixed-model line balancing using integer programming. Makssoud et al. (2014, 2015) contributed models aiming to minimize equipment investment and line modifications. Addressing disruptions, Sancı and Azizoglu (2017) proposed both a branch-and-bound method and a mixed-integer programming (MIP) approach to manage workstation failures. Zhang et al. (2018) addressed the two-sided assembly line re-balancing problem by considering changes in production demand, alterations to the line's configuration, and the production process, while Serin et al. (2019) proposed a genetic algorithm approach for U-type assembly line re-balancing problem considering stochastic task times. A comprehensive review by Cimen et al. (2022) synthesized insights from 41 studies and found that most rebalancing efforts still focus on deterministic, single-model, straight-line configurations.

Their review emphasized the lack of attention to uncertainty and alternative line structures such as U-shaped or two-sided layouts, highlighting the need for more realistic models that can capture task variability, layout complexity, and evolving system conditions.

In contrast to assembly lines, the rebalancing of disassembly lines remains a largely unexplored area, despite the increasing importance of disassembly in sustainable manufacturing and e-waste processing. The general Disassembly Line Balancing (DLB) problem has been studied using a wide array of methods, Gungor and Gupta (1999) were among the first to formalize the disassembly line balancing problem (DLBP), recognizing its inherent complexity and difference from conventional assembly lines. Over time, numerous metaheuristic techniques have been introduced to cope with DLBP's NP-complete nature, as proven by McGovern and Gupta (2007). These include the genetic algorithm (McGovern and Gupta, 2007), simulated annealing (Kalayci and Gupta, 2013a), ant colony optimization (Ding et al., 2010; Kalayci and Gupta, 2013b), particle swarm optimization (Xiao and Nie, 2017), and other swarm intelligence approaches (Zhang et al., 2017; Kalayci and Gupta, 2013c). Mathematical models have also played a significant role in the DLBP literature. Altekin et al. (2008) introduced a mixed-integer programming (MIP) model to maximize disassembly profit. Koc et al. (2009) used AND/OR graphs to represent task relationships, expanding the modeling scope. Paksoy et al. (2013) integrated fuzzy parameters into DLBP models. Later, Mete et al. (2016b, 2018) proposed novel formulations. Recent contributions emphasize sustainability, resource efficiency, and multi-objective optimization (e.g., Xu and Han, 2023; Yılmaz and Yazıcı, 2022). The literature on DLBP is broad, interested readers are referred to Özceylan et al. (2018) for a comprehensive survey on DLBP models and solution algorithms.

Despite the breadth of research on DLB, the disassembly line rebalancing problem (DLRBP) remains an underdeveloped subfield. To date, only a limited number of studies -specifically three- have addressed this gap.

Altekin and Akkan (2012) were among the first to address this problem proposing a predictive–reactive rebalancing model triggered by task failures using a predictive–reactive mixed-integer programming model allowing the system to anticipate potential failures and respond to them once they occurred. Although their approach demonstrated improved responsiveness compared to static models, it remained limited to single-period adjustments, without accounting for how previous rebalancing actions might influence future configurations.

Mete et al. (2019) extended the scope of rebalancing by introducing a mixed-integer programming model that explicitly considered supply variations in disassembly operations. In their framework, reconfiguration decisions were driven by the availability and condition of returned products, reflecting a more realistic operational context. This study provided valuable insights into how fluctuations in return flow impact line balancing efficiency; however, similar to prior work, it treated each rebalancing instance as an independent optimization problem, not considering any historical evolution of the line layout.

Wang et al. (2025) recently applied a multi-objective genetic algorithm based on Q-learning for energy-efficient e-waste disassembly line balancing and rebalancing, explicitly considering task failures. Their work represents a significant step toward integrating machine learning and metaheuristic techniques into the DLRB context, allowing adaptive decision-making under uncertainty. Nevertheless, their model, like previous ones, remains reactive in nature.

Despite these efforts, all existing studies treat rebalancing as isolated or reactive, without considering the temporal dependency between configurations. Therefore, there remains a critical need for research that incorporates multi-period, stochastic, and path-dependent rebalancing frameworks which is a gap that this thesis aims to address through its proposed model.

Table 2.1 Summary of the relevant literature on line rebalancing

Reference	Problem Type		Line Layout			Task Time Variability		Scope	Rebalancing Strategy	
	ALRB	DLRB	S	U	T-S	DTR	STC		IND	P-D
Gamberini et al. (2006, 2009)	✓		✓				✓	TOPSIS, Heuristics.	✓	
Corominas et al. (2008)	✓		✓			✓		Binary linear programming (LP)	✓	
Altemeier et al. (2009)	✓		✓			✓		Mathematical optimization	✓	
Ağpak (2010)	✓		✓	✓		✓		COMSOAL-based heuristic	✓	
Oliveira et al. (2012)	✓		✓			✓		Branch and bound, Heuristic	✓	
Yang et al. (2013)	✓		✓			✓		Multi-Objective GA, Local Search	✓	
Çelik et al. (2014)	✓			✓			✓	Ant colony optimization (ACO)	✓	
Zha and Yu (2014)	✓			✓		✓		Filtered beam search, Hybrid ACO	✓	
Makssoud et al. (2014, 2015)	✓		✓			✓		Mixed-integer LP	✓	
Sancı and Azizoglu (2017)	✓		✓			✓		MILP, Branch and bound	✓	
Zhang et al. (2018)	✓				✓	✓		Modified nondominated sorting GA	✓	
Serin et al. (2019)	✓			✓			✓	Genetic Algorithm (GA)	✓	
Altekin and Akkan (2012)		✓	✓			✓		Mixed-integer programming	✓	
Mete et al. (2019)		✓	✓			✓		Mixed-integer programming	✓	
Wang et al. (2025)		✓	✓			✓		Q-learning based multi-objective GA	✓	
This Work		✓		✓			✓	Mixed-integer NLP		✓

ALRB: Assembly line rebalancing; DLRB: disassembly line rebalancing; S: Straight; U: U-shaped; T-S: Two-sided; DTR: Deterministic; STC: Stochastic; IND: Independent; P-D: Path-dependent.

Table 2.1 presents a comparative summary of the relevant literature on line rebalancing. As shown, prior studies treat each rebalancing decision independently, meaning that the system is re-optimized from a fixed configuration every time a disruption or change occurs, without accounting for how previous layouts influence current decisions (Figure 2.1). In these approaches, the line is effectively "reset" after each disruption, assuming that the system can be reconfigured from its initial balanced state regardless of past modifications. While such methods simplify model formulation and computation, they fail to reflect the continuous and cumulative nature of real industrial environments, where previous adjustments shape the feasible options and costs associated with future reconfigurations.

As highlighted also in Cimen et al. (2022) review, the aforementioned assembly line rebalancing studies consider reassignment in the objective function by comparing each rebalanced solution to a fixed, pre-balanced configuration. This approach implicitly assumes that system conditions are static, thereby overlooking the evolutionary behavior of production systems where changes accumulate over time due to labor learning, workstation modifications, or task reallocation.

In contrast, the current study adopts a path-dependent framework in which each rebalancing step is based on the prior period's configuration, thereby capturing the temporal dynamics of real-world line adaptation. This structure allows the model to represent how operational changes in one period influence the starting point and decision space in subsequent periods. Such an approach is particularly valuable for dynamic disassembly systems, where reconfigurations are often constrained by physical layouts, cost limitations, and workforce continuity. By integrating this sequential and dependent perspective, the proposed framework provides a more realistic depiction of how disassembly lines evolve over time, offering improved decision support for sustainable and flexible rebalancing under uncertainty.

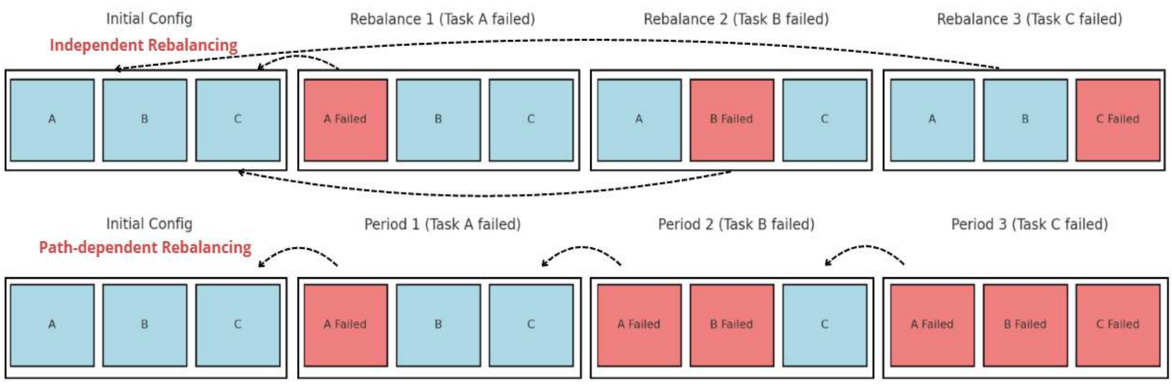

Figure 2.1 Independent vs. path-dependent rebalancing approach

Figure 2.1 illustrates the difference between the independent and path-dependent rebalancing strategies in disassembly line operations, showing how in the independent rebalancing strategy the initial configuration is used as a reference point and repeatedly reconfigured whenever a disruption occurs (say a task fails), without considering prior adjustments making every adjustment independent of the other. For example, when task A failed in the line, the line was reconfigured based on the initial configuration. Later, when task B failed, the line is again reconfigured based on that same initial configuration, and so on. This makes the line rebalanced separately in each task failure scenario and optimized as a one-time adjustment, neglecting what happened in the past. While this method may simplify the rebalancing process, it overlooks the cumulative impact of previous disruptions and adjustments, making it less reflective of how manufacturing systems evolve over time in real-life. On the other hand, the proposed path-dependent approach introduces a more realistic and connected approach, reflecting the idea that decisions and adjustments are connected; past adjustments shape future ones. Thus, here, each rebalancing decision builds upon the configuration that resulted from previous adjustments. Therefore, when task A failed in the line in Figure 2.1, the line in the first period was rebalanced based on the previous period, – in this case the initial configuration- while later when task B failed in period 2, the line is now rebalanced taking into consideration the configuration established in period 1, and not the initial configuration. This means that every change in the line’s structure influences future configurations, creating a sequence of dependent decisions that better represents real-world industrial practices. In actual production environments, physical constraints, cost limitations, and workforce continuity often prevent the system from being fully reset to its original state after each disruption. The path-dependent strategy, therefore, captures the nature of line configurations evolves over time.

Hence, building on this foundation, the proposed work fills a critical gap in the line rebalancing and specifically in the disassembly domain literature by integrating three critical elements:

- ✓ sequential multi-period,
- ✓ stochastic,
- ✓ and U-shaped layout characteristics

In the context of disassembly line rebalancing. This novel combination contributes a more realistic, adaptive, and robust decision-making framework for dynamic remanufacturing environments, which is a one that aligns closely with the complex, uncertain, and evolving nature of real disassembly systems.

CHAPTER 3
PROBLEM DEFINITION

In modern remanufacturing and sustainable production systems, disassembly lines play a central role in the reuse of EoL products. Unlike the traditional assembly systems that focus on product construction, disassembly lines are designed to dismantle complex products into their constituent components and materials in a systematic way, enabling the extraction of reusable parts, recycling of valuable materials, and ensuring a safe disposal of hazardous or non-recyclable components. However, the operational environment of disassembly systems is considered as more complex than that of traditional assembly lines. This complexity is due to the inherent uncertainty that is associated with the returned products, variations in product condition and composition. Thus, such variations can lead to unpredictable task times, uncertain disassembly task sequences, and even external factors such as fluctuations in supply and demand of returned products, further complicating the planning and balancing of disassembly lines. Therefore, disassembly lines must be designed and balanced in a way that ensures flexibility, efficiency, and adaptability to accommodate such uncertain conditions and challenges.

Among various disassembly line configurations, the U-shaped disassembly line has received increasing attention due to its flexibility and improved line balancing potential compared to traditional straight lines (Agrawal & Tiwari, 2008; Avikal & Mishra, 2012; Avikal et al., 2013). The U-shaped configuration allows tasks to be assigned to both the entrance and exit sides of the line, enabling workers to perform operations from both directions. Thus, such characteristic offers greater task assignment flexibility which allows a more balanced distribution of workload among stations, thereby reducing idle time, improving overall line efficiency, and providing better adaptability to complex task precedence relationships.

Figure 3.1 illustrates the U-shaped disassembly line layout adopted in this thesis. As shown in Figure 3.1, tasks can be assigned to both the front (entrance) and back (exit) sides of each station in a U-shaped layout, allowing operators to work from either direction. This bidirectional accessibility facilitates more compact line configurations, improved operator utilization, and greater adaptability to complex precedence relationships in which these features are particularly advantageous in disassembly systems where task variability and uncertainty are common.

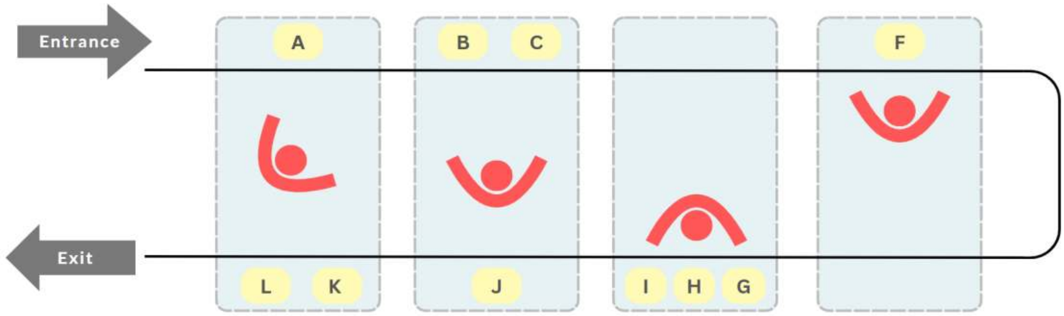

Figure 3.1 Layout of the U-shaped disassembly line

Figure 3.2 shows a comparison between task assignments solution for a traditional straight disassembly line vs. a U-shaped disassembly line. Both solved under the same parameters with a cycle time of 20 units for an 8-task example adapted from Li et al. (2021). As observed in Figure 3.2 (a), the straight line requires five stations to execute all tasks while satisfying precedence and cycle time constraints.

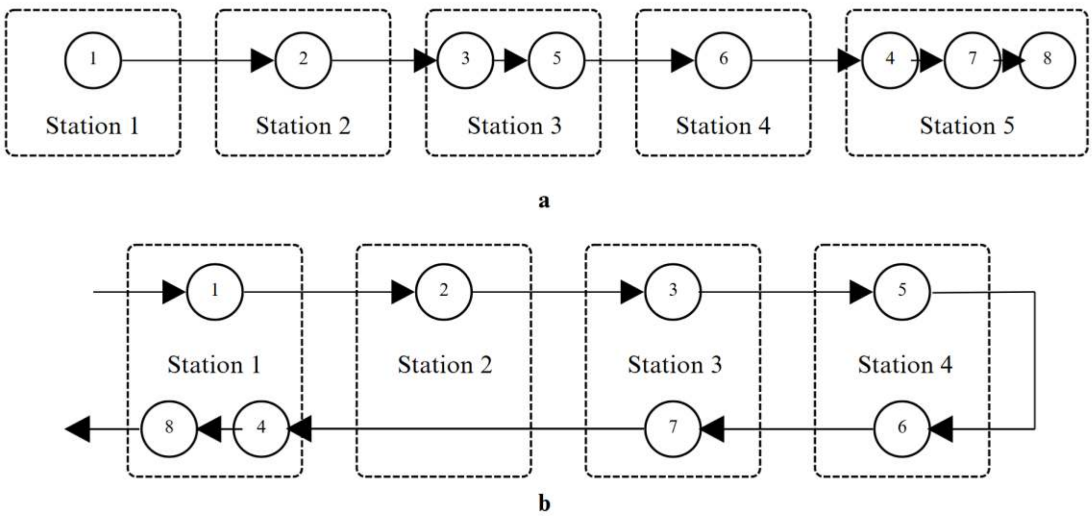

Figure 3.2 Traditional (a) and U-type disassembly line (b) with a cycle time of 20

In contrast in Figure 3.2 (b), the U-shaped layout achieves the same disassembly objectives using only four stations. This reduction in the number of required stations highlights one of the key advantages of the U-shaped layout, which is the enhanced station utilization. The improvement stems from the bidirectional accessibility of U-shaped lines that allow tasks to be assigned in a more flexible and compact manner. For example, the operator at Station 1 performs task 1 on the entrance side, followed by tasks 4 and 8 on the exit side. At Station 4, the operator begins with task 5 on the entrance side and then proceeds to task 6 on the exit side. This feature effectively expands the task assignment space, enabling better grouping of tasks with complementary processing times, and reducing idle time within stations.

In today's competitive and dynamic production environment, companies involved in product recovery, remanufacturing, and recycling must remain flexible and responsive to customer needs and environmental requirements. As lead times shrink and disassembled products vary in type and condition, fluctuations in product return volumes and component demanded can disrupt the balance of the disassembly line. Such disruptions often reduce productivity, increase idle time, and lead to inefficiencies in the utilization of labor and resources.

Consequently, the process of eliminating an existing system and building another one from zero to accommodate these variations is both costly and time-consuming. Instead, it is more practical to reconfigure the current line to satisfy the changing operational requirements. This process is referred to as line rebalancing. Line rebalancing is the process of modifying an existing line configuration (the task-to-station assignment) to adapt to changes in demand/supply, product design, task times, number of workstations, or cycle time, while maintaining or improving the efficiency and balance among stations where the line became to a point that is no longer efficient or feasible under such changing conditions.

In this study, rebalancing is considered as the reallocation of disassembly tasks to different stations across multiple periods, where each rebalancing event is triggered by demand-driven changes in cycle time. This means, as demand fluctuates, the required cycle time changes accordingly: higher demand leads to tighter cycle times and perhaps additional workstations, while conversely, lower demand allows longer cycle times and potential station consolidations.

This thesis therefore focuses on cycle time variability as the primary rebalancing trigger. Unlike conventional approaches that treat each rebalancing instance independently as an isolated event, we propose a MILP model incorporating a path-dependent rebalancing framework in which the line retains a “memory” of its prior configurations where each rebalancing period begins from the previous period’s configuration rather than resetting and going back to an initial baseline, and changes such as task relocations or station adjustments incur explicit rebalancing costs. As a result, rebalancing decisions are influenced by both current constraints and historical configurations, capturing how real disassembly systems evolve over time.

The primary objective of the proposed model is to determine the optimal sequence of task-to-station assignments that minimizes total rebalancing cost (RC), which includes task relocation and workstation operating costs. To address the uncertainty in disassembly task durations, the model incorporates a stochastic formulation using a chance-constrained approach. In this framework, task times are modeled as normally distributed random variables with known means and variances, and the chance constraints ensure that the probability of violating the cycle time per station remains below a predefined confidence level.

Through this integrated approach, the proposed model provides a realistic decision-making framework that reflects the operational, temporal, and stochastic complexities in modern disassembly environments. It helps practitioners to plan adaptive, cost-effective, and sustainable rebalancing strategies that maintain high efficiency and resilience across multiple periods.

The proposed model is based on the following assumptions:

- A single product type is completely disassembled on the U-shaped line.
- The precedence relations between the tasks are known.
- Task times are stochastic and normally distributed with known parameters.
- Each task's location in the line is determined based on the configuration from the previous period; relocation may incur a cost (Relocation cost).
- Task relocation costs are randomly generated within a defined range.
- Opening a new workstation involves a fixed operating cost.

3.1 Model Formulation

In a U-shaped disassembly line, the product moves along a bidirectional path: it begins at the entrance side of the first station, proceeds forward through successive entrance-side sub-stations until the last, and then returns along the exit side, moving from the last station back toward the first station. This flow structure, as illustrated in Figure 3.3, is adapted from the encoding logic of Li et al. (2021). To capture this U-shaped layout mathematically, each station is modeled as having two sub-stations: those on the entrance side, indexed as 1, 2, …, M and those on the exit side, indexed as M+1, ⋯, 2M-1, 2M as illustrated in Figure 3.3. Therefore, a product is disassembled in the sequence of sub-stations 1,2, ⋯, M then substation M+1, ⋯, 2M, following the natural flow of the U-line. Based on that, the proposed MILP model will be formulated following the encoding and processing order of the U-line adopted in Figure 3.3.

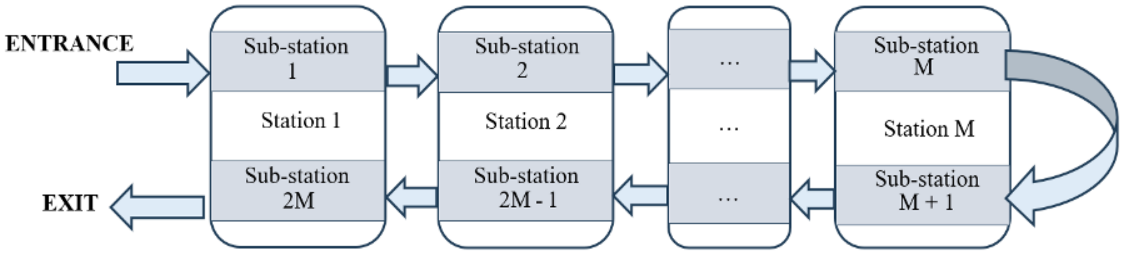

Figure 3.3 The encoding and indexes of the sub-stations

In the considered stochastic disassembly line rebalancing (SDLRB) problem, the solution must satisfy both precedence constraints and a chance-constrained cycle time limitation to ensure that, the probability of the total processing time at any workstation exceeding the selected cycle time remains within an acceptable confidence level.

The proposed model is established following the model logic of Mete et al. (2019) and Li et al. (2021), where our model is formulated to follow a U-shaped line and the main objective is to minimize the total rebalancing costs imposed by demand variations. In addition, our model is extended to include a memory embedded to the line to reflect the concept of path-dependency.

The complete mathematical formulation of the proposed MILP model, including its constraints, is presented in expressions (1-8) and the notations are given as follows:

Indices

N	Total number of tasks (or parts)
i, j	Task indices, $i, j = 1,2, \cdots, N$
M	Maximum number of allowed opened stations
m, n	Sub-station indices, $m, n = 1,2, \cdots, 2M$
p	Rebalancing period index, $p = 1,2, \dots, P$

Parameters

CT_{p-1}	Cycle time for the initial line balance and rebalancing periods $p - 1$
CT_l	New cycle time in rebalancing period p
μ_i	Mean time of task i
σ_i	Standard deviation of task i
$z_{1-\alpha}$	z-score for confidence level α
W_n	Set of tasks assigned to main station m
ANDP (i)	Set of AND predecessors of task i
ORP (i)	Set of OR predecessors of task i
ORPT	Set of tasks which have OR predecessors
$Cost_1$	Operating cost of workstation
$Cost_2^p$	Cost incurred if task i is assigned to main station m in period p, given that it was located elsewhere in period p-1 (relocation cost)
A_{im}^{p-1}	1, if task i was assigned to main station m in period p-1, 0, otherwise

Decision variables

x_{im}	1, if task i is allocated to the sub-station m; 0, otherwise
y_{im}	1, if task i is allocated to the main station m; 0, otherwise
C_{im}^p	1 if task i is assigned to main station m in the current period p, but not assigned to the same station in period p-1
z_m	1, if the main station m is opened; 0, otherwise

The objective function, presented in Equation (1), minimizes the total weighted rebalancing cost, combining the operating cost of opened workstations (weighted by w_1) and the task relocation cost (weighted by w_2) incurred when a task changes station between periods.

$$\text{Min } = w_1 . Cost_1 . \sum_{m=1}^{M} Z_m + w_2 . Cost_2^p . \sum_{i=1}^{N} \sum_{m=1}^{M} C_{im}^p \cdot y_{im} \tag{1}$$

$$\sum_{m}^{M} (x_{im} + x_{i,2M+1-m}) = 1 \quad \forall i \tag{2}$$

$$y_{im} = \sum_{m=1}^{M} (x_{im} + x_{i,2M+1-m}) \quad \forall i, m \tag{3}$$

$$C_{im}^p = y_{im} . (1 - A_{im}^{p-1}) \quad \forall i, m \tag{4}$$

$$P \left\{ \sum_{i \in W_m} \mu_i \ + \ z_{1-\alpha} . \sum_{i \in W_m} \sigma_i \ \le z_m \cdot CT_p \right\} \ge 1 - \alpha \ \ \forall m \tag{5}$$

$$x_{im} \le \sum_{n=1}^{m} x_{jn} \quad \forall m, i \text{ , and } j \in \text{ANDP}(i) \tag{6}$$

$$x_{im} \le \sum_{j \in \text{ORP}(i)} \sum_{n=1}^{m} x_{jn} \quad \forall m, i \in \text{ORPT} \tag{7}$$

$$x_{im}, y_{im}, C_{im}^p, z_m \in \{0,1\} \ \ \forall i, m \tag{8}$$

Equation (2) ensures that each task is assigned to exactly one sub-station (either to the entrance or exit sub-station). Equation (3) links sub-station assignments to their corresponding main stations. Equation (4) is the memory constraint, which enables path dependency in the model. It ensures that only actual task relocations are penalized i.e., when a task is newly assigned to main station m in period p but was not assigned there in period $p-1$. Equation (5) introduces the chance-constrained cycle time, enforcing a probabilistic upper bound on the total task time within each main station. Specifically, the sum of mean task durations plus a safety margin (based on the standard deviation and desired confidence level) must not exceed the available cycle time. Equation (6) ensures that a task can only be assigned if all of its AND predecessors have already been allocated to either earlier sub-stations or prior positions within the same sub-station. Equation (7) ensures that a task can be assigned once at least one of its OR predecessors has been allocated to a preceding sub-station or an earlier position within the same sub-station. Equation (8) enforces the binary nature of decision variables.

This formulation captures the complexity and uncertainty of real-life disassembly systems by integrating:

- Stochastic modeling of task durations
- Chance constraint for probabilistic reliability
- U-shaped layout logic for improved station utilization
- Sequential memory for cost-aware rebalancing decisions

By including explicit costs and probabilistic feasibility conditions, the model offers a tool for practitioners facing dynamic demand and uncertain task performance. The methodology adopted in this thesis is presented in Chapter 4.

CHAPTER 4
METHODOLOGY

This chapter presents the methodological framework developed to model the multi-period sequential rebalancing of a U-shaped disassembly line under stochastic task durations. The proposed model reflects the dynamic nature of disassembly systems, where each rebalancing period is influenced by the task-to-station configuration of the previous period, introducing the concept of path dependency. This sequential decision-making structure ensures that rebalancing events consider both current conditions and the historical configuration of the line, leading to more realistic and cost-effective rebalancing outcomes.

4.1 Stochastic modeling framework

In both stochastic line balancing and U-line balancing problems, task durations are treated as random variables with known probability distributions. In the literature, task times are usually assumed to follow a normal distribution, defined by a known mean and variance for each task. This is because task times are influenced by many small, independent factors (For example, worker speed, machine variability, delays, etc.), and the sum of these small independent variations tends to follow a normal distribution according to the Central Limit Theorem. Thus, each task i (where i =1, …, N), is modeled as an independent stochastic variable, with mean μ_i and variance σ_i^2. To ensure reliable operation under uncertainty, we imposed a chance constraint which require that the probability of completing all tasks assigned to a workstation within the allowed cycle time is no less than a confidence level (1−α), (Chiang and Urban, 2006). This is formally represented as:

$$P\left\{\sum_{i\in W_m} \mu_i + z_{1-\alpha}\sqrt{\sum_{i\in W_m} \sigma_i^2} \le z_m \cdot CT_p \right\} \ge 1-\alpha \ \forall m$$

where W_m represents the set of tasks assigned to workstation m, CT_p denotes the cycle time in period p, and $z_{(1-\alpha)}$ is the critical value from the standard normal distribution corresponding to the confidence level $(1-\alpha)$.

This chance-constrained formulation ensures that each station's total expected processing time, along side with a safety margin which is determined by the variability of task times, remains within the cycle time with the desired level of confidence. As the variability (or uncertainty) in task times increases, the safety margin also expands, making the model more conservative but also more robust against uncertainty.

However, while the chance constraint provides a realistic representation for the stochastic behavior, it introduces nonlinearity due to the standard deviation term $\sqrt{\sum \sigma_i^2}$, which can significantly increase computational complexity, especially for large-scale problems. Thus, to ensure tractability in the model, a linear approximation is applied to the nonlinear standard deviation term in the chance constraint to improve computational tractability. Specifically, the standard deviation term $\sqrt{\sum \sigma_i^2}$ is replaced by its linear upper bound $\sum \sigma_i$ (see Eq. (5) in chapter 3.1), following the approach adopted in the literature (e.g., Özcan, U., 2009).

This approximation ensures retaining conservativeness in constraint satisfaction, ensuring that feasible solutions under the linearized form remain feasible under the original nonlinear constraint and reduces solver complexity, while preserving the model's ability to capture stochastic variability under chance-constrained requirements.

4.2 Illustrative example

This section demonstrates the solution of a small-sized benchmark instance (P10-OR) involving 10 disassembly tasks, reported in Ren et al. (2017). The precedence relationships among tasks are illustrated in Figure 4.1, which includes 10 actual tasks and one dummy task, labeled A1. The dummy task is used to simplify the modeling of OR precedence relations. Specifically, task A1 can be processed once either task 2 or task 3 has been completed. Unlike real tasks, task A1 has zero processing time. The deterministic task durations of the P10-OR instance are provided in Table 4.1.

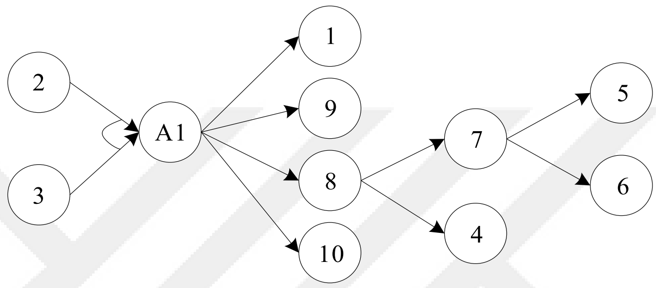

Figure 4.1 Precedence diagram of P10-OR by Ren et al. (2017)

Firstly, an initial deterministic U-shaped disassembly line balance is established for a predefined cycle time (CT_0) of 60 seconds. The objective at this stage is to minimize the number of workstations while ensuring that all tasks are assigned in compliance with both precedence constraints and the imposed cycle time limits. In this case, the cycle time constraint ensures that the total processing time on either the entrance or exit side of each station does not exceed the specified cycle time. While the precedence constraints require that a task may only be executed once all of its AND predecessors have been completed, or once at least one of its OR predecessors has been removed.

Table 4.1 Task times of the P10-OR

Task No.	Part removal time
1	14
2	10
3	12
4	18
5	23
6	16
7	20
8	36
9	14
10	10

The optimal task assignment obtained for the P10-OR instance is shown in Figure 4.2. As illustrated in Figure 4.2, the initial balance is established with the model opening three stations and tasks are assigned to both sides of each station aligning with the U-shaped layout of the line, where operators can perform tasks on both sides of the line.

The deterministic balance obtained at this stage will serve as the baseline configuration for the subsequent rebalancing experiments for each scenario. It represents the system's starting point before introducing stochastic variability and multi-period adjustments, forming the foundation for the path-dependent rebalancing process.

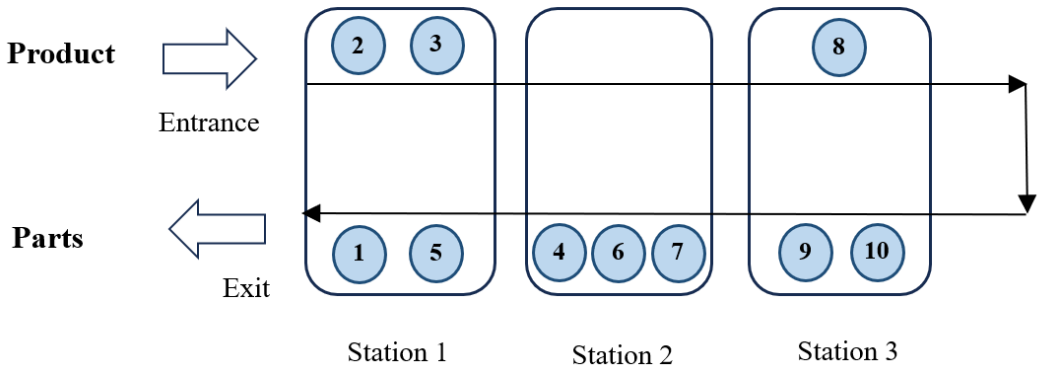

Figure 4.2 Initial line configuration for the P10-OR ($CT_0 = 60$)

For the U-shaped disassembly line presented in this study, rebalancing becomes necessary due to fluctuations in customer demand, which directly impact the cycle time across planning periods. As demand increases, the cycle time must be reduced to maintain throughput to satisfy the increased demand, which often require the addition of workstations. Conversely, lower demand allows for cycle time relaxation, enabling task consolidation and potential station closures. These demand-driven changes the task-to-station assignments, thereby introducing rebalancing costs, which consist of task relocation costs and workstation operating costs.

The goal is to reconfigure the line in each period sequentially to adapt to the updated cycle time while minimizing the total rebalancing cost. Task relocation costs are incurred whenever tasks are reassigned to different stations compared to the previous configuration, and operating costs are tied to the number of active workstations. In this study, we assume a one-month planning horizon for each period, thus each opened station is associated with a fixed monthly operating cost.

This framework aligns with practical industrial settings where fully reconstructing a disassembly line is unpractical, and iterative reconfiguration offers a more cost-effective and adaptable solution that help decision-makers make more informative decisions instead of relying on just a one-time optimal solution.

After establishing the initial line configuration, the model incorporates stochastic task durations to reflect real-world variability in disassembly operations. The deterministic task times of the P10-OR are now assumed as mean values (μ_i) of normally distributed stochastic task durations, while the corresponding variances are derived using predefined coefficients of variation (CV), this means that the standard deviation for each task is computed as $\sigma i = \mathrm{CV} \times \mu_i$. In line with Silverman and Carter (1986), two levels of variability are used to simulate different uncertainty conditions: CV = 0.10 for low variance and CV = 0.25 for high variance environments.

Figure 4.3 illustrates the first rebalancing period for the P10-OR instance under a high demand scenario, where the cycle time is reduced to $CT_1 = 55$ seconds. As shown, four workstations are opened to accommodate the increased workload. Notably, tasks 5, 7, and 9 are reassigned to different stations compared to their positions in the initial configuration in Figure 4. Noting that these relocations are necessary to satisfy the updated cycle time and precedence constraints, contributing to the overall rebalancing cost.

To model the cost structure realistically, the planning parameters of the paper are taken considered as proposed by Celik et al. (2014) and Serin et al. (2019). A one-month planning horizon is considered. During this period, each opened workstation incurs a fixed operating cost of $2000. In addition, task relocation costs are included to demonstrate the expense of reassigning a task to a different station compared to its previous configuration.

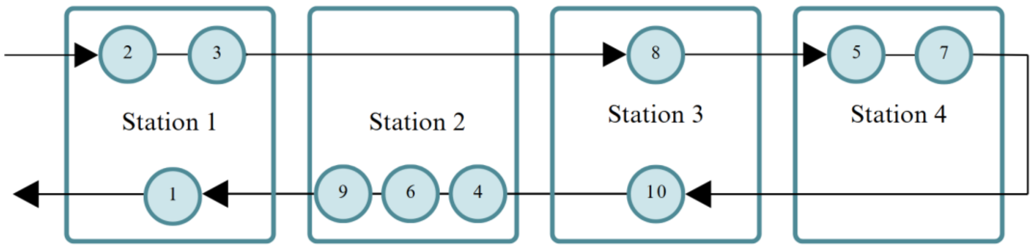

Figure 4.3 The rebalanced line configuration for the P10-OR ($CT_1 = 55, CV = 0.1, \alpha = 0.90$)

Table 4.2 shows the relocation costs of the P10-OR instance tasks when reassigned to different stations. As it can be seen, there are 10 tasks and 10 stations and each task is assigned a relocation cost when it changes location in the upcoming periods. The relocation costs are randomly generated within a range of $200 to $2000, reflecting variable equipment and labor handling requirements. The zero values indicate the location of the task in the previous period. In other words, if a task has retained its previous location in the current rebalancing period, no reassignment occurs, and thus no relocation cost is incurred for that task. The relocation cost matrix is updated after each rebalancing period based on the comparison of current task assignments with the previous period. This updating process allows the model to track the evolution of task positions over time and calculate corresponding cost implications for each rebalancing step. It also shows the path-dependent structure of the model, whereby each decision is influenced by prior configurations.

Table 4.2 Task relocation costs ($) of the P10-OR instance

Task No.	Station No.									
	S1	**S2**	**S3**	**S4**	**S5**	**S6**	**S7**	**S8**	**S9**	**S10**
1	0	1621	1621	1621	1621	1621	1621	1621	1621	1621
2	0	1956	1956	1956	1956	1956	1956	1956	1956	1956
3	0	1613	1613	1613	1613	1613	1613	1613	1613	1613
4	684	0	684	684	684	684	684	684	684	684
5	0	232	232	232	232	232	232	232	232	232
6	301	0	301	301	301	301	301	301	301	301
7	1562	0	1562	1562	1562	1562	1562	1562	1562	1562
8	1713	1713	1713	0	1713	1713	1713	1713	1713	1713
9	1355	1355	1355	0	1355	1355	1355	1355	1355	1355
10	1075	1075	1075	0	1075	1075	1075	1075	1075	1075

Both cost components -station operating cost and task relocation cost- are integrated into the objective function using weight parameters w_1 and w_2, representing the relative importance of workstation operating cost and relocation cost, respectively. In this study, equal weights are assigned to both components ($w_1 = w_2 = 0.5$) for demonstration purposes; however, these weights can be adjusted by decision-makers to reflect specific operational priorities. For example, industries with high relocation costs due to hazardous material handling may prioritize minimizing reassignments, while others may focus on limiting the number of active stations to save on fixed overhead.

To evaluate the performance of the model under dynamic conditions, three demand-driven scenarios are defined based on varying cycle times across four rebalancing periods. For the P10-OR instance with an initial cycle time of 60 seconds, the high-demand scenario includes decreasing cycle times (e.g., 55 → 50 → 45 → 41), reflecting increased production pressure and tighter cycle times to accommodate it. The low-demand scenario adopts increasing cycle times (e.g., 65 → 71 → 77 → 83), simulating more relaxed operational conditions and cycle times. Lastly, the cyclical demand scenario alternates cycle times to mimic fluctuating market conditions (e.g., 55 → 65 → 50 → 60).

For each scenario, the model is tested under two levels of task time variability, a low CV = 0.10 and a high CV = 0.25, combined with three confidence levels α (0.90, 0.95, 0.975) used in the chance-constraint formulation. This setup allows the examination of how different combinations of uncertainty and levels of confidence impact the rebalancing behavior. In total, this results in 24 rebalancing runs per scenario, in addition to the initial balance, leading to a total of 73 model runs per problem instance.

Each run produces key outputs, including the total rebalancing cost (RC), number of stations opened (NS), and the CPU time. These results are analyzed and discussed in Chapter 5 to assess the experimental design and how the model adapts to varying levels of uncertainty and operational demands.

CHAPTER 5
RESULTS AND DISCUSSION

This section presents and discusses the experimental design established for this study, along with the computational results obtained from applying the developed model and a comparative analysis to evaluate the effectiveness of the proposed approach.

The performance of the developed MILP model is tested by solving six instances from the literature presented in Table 5.1. The naming of the instances in Table 5.1 denotes the number of tasks in each problem instance, while the suffix "OR" signifies the inclusion of AND/OR precedence relations. These instances were chosen to test the model's capability to handle different problem sizes and varying structural complexities.

For the P22-OR, P34-OR, P47-OR, P60-OR, and P73-OR instances, the original task operation times were not specified in Kalaycılar et al. (2016). To address this, this study assigns new processing times for the tasks by sampling from a discrete uniform distribution over the interval [1,20] following the same approach of Kalaycılar et al. (2016) in their paper. In addition, we generated the P133-OR instance on our own by combining the precedence relations of P60-OR and P73-OR.

Table 5.1 The tested problem instances obtained from the literature

Instance	Description
P10-OR	The instance with 10 tasks reported in Ren et al. (2017).
P22-OR	The instance modified from ball-point pen with 22 tasks by Kalaycılar et al. (2016).
P47-OR	The instance with 47 tasks by Kalaycılar et al. (2016).
P60-OR	The instance with 60 tasks by Kalaycılar et al. (2016).
P73-OR	The instance with 73 tasks by Kalaycılar et al. (2016).
P133-OR	Generated by combing the precedence relations of P60-OR and P73-OR.

5.1 Experimental design

In the literature, the commonly adopted confidence levels for chance-constrained line balancing problems are 0.90, 0.95, and 0.975, as reported by Celik et al. (2014), Baykasoğlu and Özbakır (2007), Chiang and Urban (2006), Bagher et al. (2011), Foroughi et al. (2016), and Mete et al. (2019). In line with these studies, our present work also evaluates model performance under the same three confidence levels, and task durations are modeled based on normally distributed random variables, reflecting the probabilistic nature of task times in real-world disassembly processes.

To evaluate the model's performance, a comprehensive experimental setup is designed, which involve multiple demand-driven scenarios and uncertainty levels.

The process begins by generating an initial deterministic U-shaped line balance under a fixed cycle time (CT_0), serving as the starting point for all subsequent rebalancing phases. Then, the rebalancing phase starts, where the model is tested across three demand scenarios:

- High demand (decreasing cycle times),
- Low demand (increasing cycle times),
- Fluctuated (cyclical) demand (alternating cycle times).

Each demand scenario includes four rebalancing periods, with each period associated with a different cycle time (CT_p) to reflect demand fluctuations over time.

To capture the stochasticity of task times, for each scenario case, the model will be evaluated on high and low coefficients of variance (CV). In line with a study of Silverman and Carter (1986), a 0.10 for low and 0.25 for high variances will be used. This will help assess how increasing uncertainty in task durations affects the line's performance and the rebalancing solutions.

Furthermore, for each coefficient of variance (CV), the three levels of confidence α, as 0.90, 0.95, and 0.975 will be considered. Hence, 1 initial balance + (3×4×2×3) =73 test problems per instance will be generated. The model will be tested on 6 problem instances of different sizes from the literature. The six instances are solved by GAMS-DICOPT solver. Hence, 6 × 73 = 438 model runs will be obtained for the experimental analysis.

5.2 Computational results

To analyze the results more in greater depth, Table 5.2 presents the detailed outcomes of the illustrative example P10-OR under the low demand scenario results for all the settings. Table 5.2 includes columns such as, the CV level, the confidence level (1-α), Period_i representing the four-rebalancing periods, CT_{i-1} denotes the cycle time used in period $i - 1$, used as the reference point for each rebalancing decision, while CT_i is the updated cycle time reflecting current demand, RC is the rebalancing cost incurred at period i, #NS is the number of stations opened at each period, and CPU (s) is the CPU time in seconds.

Looking at Table 5.2, illustrating the low demand scenario, where the cycle time progressively increases across four rebalancing periods (from 65 to 83 seconds), the results reveal a general decline in rebalancing costs as the line becomes less constrained with longer cycle times. This trend is particularly evident under low variability conditions (CV = 0.10), where the reduced uncertainty leads to more stable and consistent task assignments. In these cases, the model requires fewer adjustments between periods, as the relaxed cycle times provide sufficient capacity to accommodate task variations without major reconfigurations.

Conversely, at a higher variability level (CV = 0.25), the model incurs higher rebalancing costs in earlier periods due to the compounded effects of uncertainty and stricter chance-constraint safety margins, which limit feasible task combinations and force additional task relocations to satisfy the probabilistic cycle time constraints. A notable pattern observed is the stabilization of the line configuration after some rebalancing periods, particularly under high variability (CV = 0.25). For example, when the confidence level is set to 90%, the model opens four workstations in the first period, incurring both relocation and operating costs. In the subsequent periods, despite continued increases in cycle time, the model maintains the same task-to-station assignments and incurs only operating costs which is highlighted in bold in the table, indicating that no further task relocations occur. This stabilization reflects the path-dependent structure of the model, showing how decisions in each period are influenced by the previous configuration and how the model adapted to this.

Table 5.2 P10-OR Scenario 2: Low Demand

CV	**1- α**	**Period$_p$**	**CT$_{p-1}$**	**CT$_p$**	**RC**	**#NS**	**CPU (s)**
0.1	90	1	60	65	$5146	4	0.125
		2	65	71	$3879.50	3	0.109
		3	71	77	**$3000**	3	0.094
		4	77	83	**$3000**	3	0.094
	95	1	60	65	$5146	4	0.125
		2	65	71	**$4000**	4	0.125
		3	71	77	$3608.50	3	0.094
		4	77	83	**$3000**	3	0.109
	97.5	1	60	65	$5146	4	0.156
		2	65	71	**$4000**	4	0.109
		3	71	77	$3608.50	3	0.140
		4	77	83	**$3000**	3	0.109
0.25	90	1	60	65	$5574.50	4	0.438
		2	65	71	**$4000**	4	0.109
		3	71	77	**$4000**	4	0.141
		4	77	83	**$4000**	4	0.125
	95	1	60	65	$5830	4	0.125
		2	65	71	**$4000**	4	0.125
		3	71	77	**$4000**	4	0.125
		4	77	83	**$4000**	4	0.109
	97.5	1	60	65	$6753.50	5	0.141
		2	65	71	**$5000**	5	0.125
		3	71	77	**$5000**	5	0.140
		4	77	83	$4492.50	4	0.125

Values in **bold indicates no task relocation. Only workstation operating costs incurred.*

Since we have firstly assigned equal weights to the objective for demonstration purposes, we have conducted a weight-sensitivity analysis. The purpose of this analysis is to examine how the model responds as the cost-weight parameters (w_1, w_2) are gradually shifted from putting full emphasis on relocation costs to prioritizing workstation operating costs. Figure 5.1 illustrates presents the results of a weight-sensitivity analysis conducted for instance P10-OR under the setting $CT_1 = 55$, $CV = 0.25$, and $\alpha = 0.90$.

The results clearly show that as the weight on relocation costs decreases, the model correspondingly allocates fewer resources toward reducing reassignments. This leads to a steady decline in relocation cost, eventually reaching zero when $w_2 = 0$ in Case 11. In contrast, workstation operating cost behaves in the opposite direction: it is extremely high in Case 1 when its weight in the objective is zero, but it drops sharply as soon as even a small positive weight is assigned to workstation cost. After this point, workstation cost stabilizes and remains nearly constant across the remaining cases. This pattern highlights an important insight: assigning even a modest weight to workstation cost encourages the solver to minimize the number of open stations early, reflecting a strong sensitivity to this cost component.

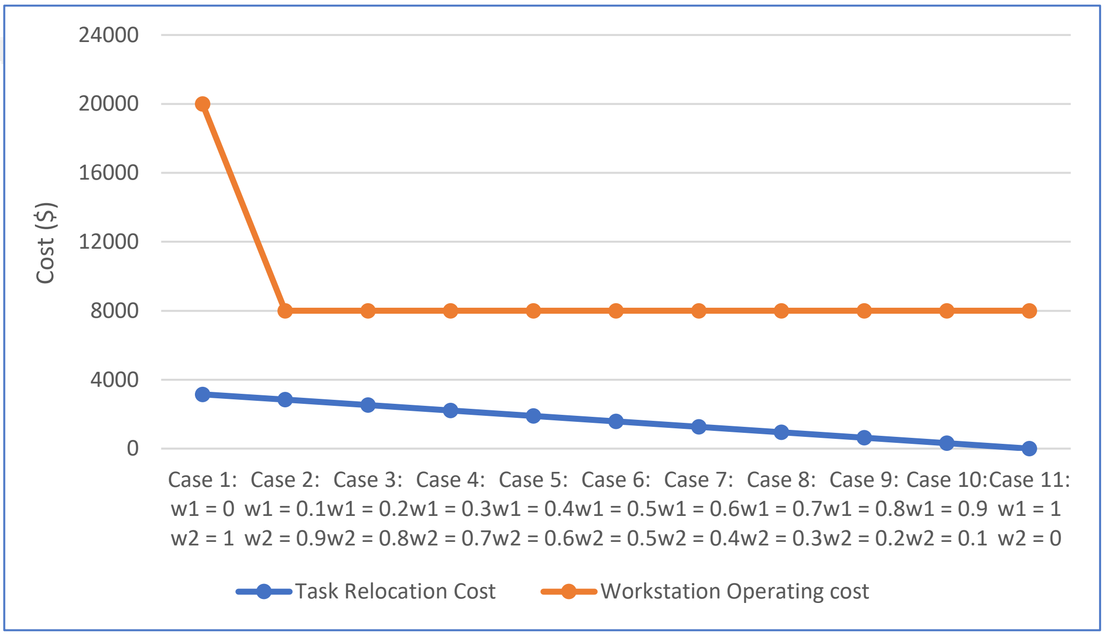

Figure 5.1 Rebalancing cost results for P10-OR

$(CT_1 = 55, CV = 0.1, \alpha = 0.90)$

Figures 5.2 and 5.3 show similar trends for higher confidence levels. As α increases, the model becomes more conservative due to the larger safety buffer required by the chance-constraint. In Figure 5.2, for example, a reduction in station operating cost in Case 4 (i.e., fewer stations being used) leads directly to a slight increase in relocation cost, indicating that consolidating tasks under greater uncertainty requires more structural adjustments.

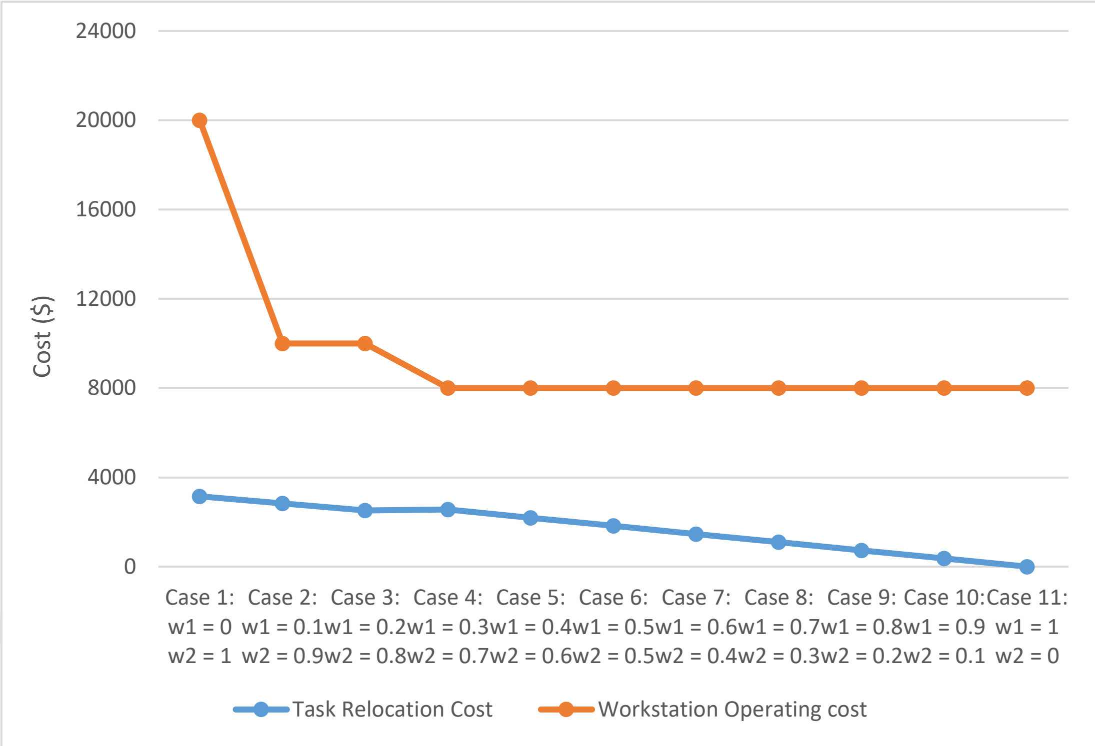

Figure 5.2 Rebalancing cost results for P10-OR

$(CT_1 = 55, CV = 0.1, \alpha = 0.95)$

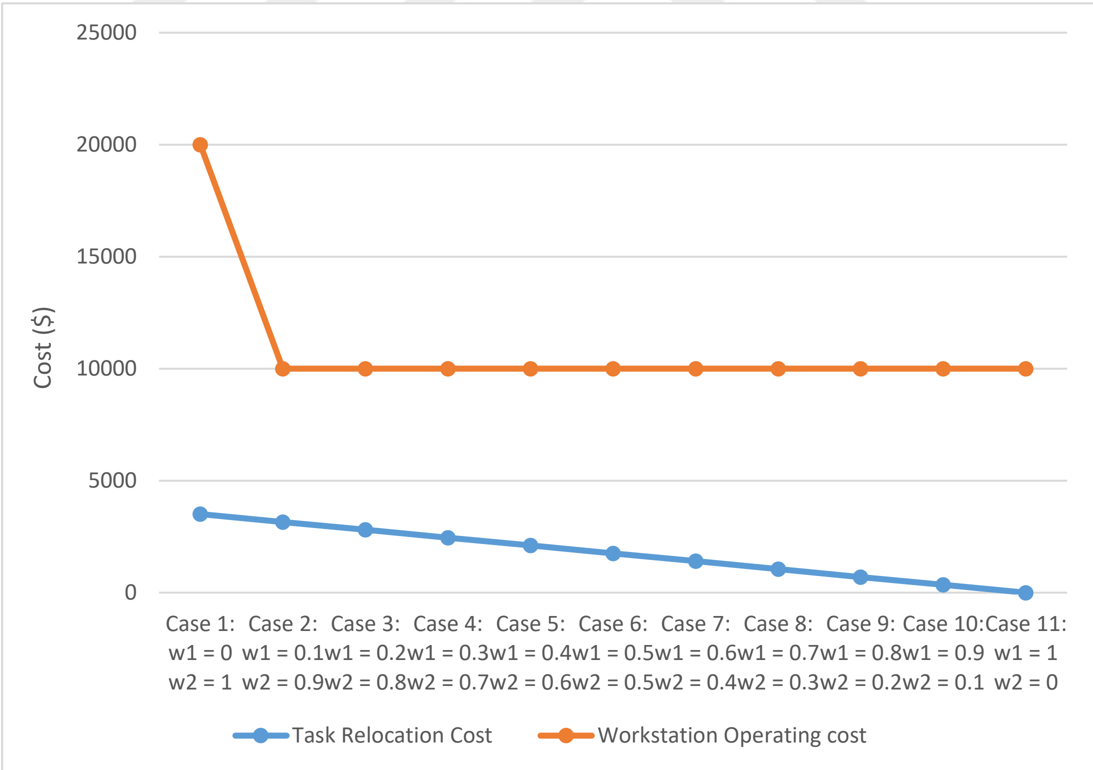

Figure 5.3 Rebalancing cost results for P10-OR

$(CT_1 = 55, CV = 0.1, \alpha = 0.975)$

Figures 5.4–5.6 present the same analysis under high variability conditions. The general behavior observed under low variability continues to be the same: as the two cost components exhibit an inherent trade-off. Reducing station operating cost typically requires consolidating tasks into fewer stations, which increases the need for relocations to achieve feasible load balancing. Conversely, minimizing relocations preserves the current layout but often results in higher operating costs due to a larger number of active stations.

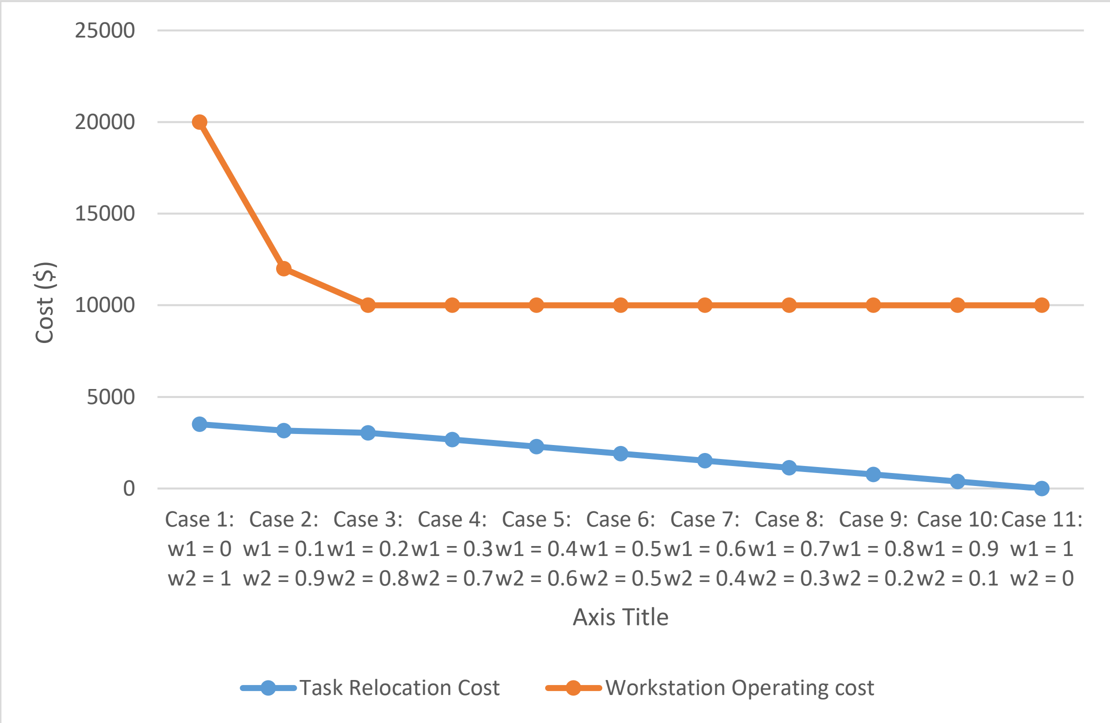

Figure 5.4 Rebalancing cost results for P10-OR

$(CT_1 = 55, CV = 0.25, \alpha = 0.90)$

Overall, the sensitivity analysis confirms that the model behaves in a predictable and managerial-meaningful way. The trade-off between relocation cost and station operating cost is structural: improving one tends to worsen the other. This implies that the choice of weights (w_1, w_2) can be guided directly by managerial priorities. If stability and minimal task movement are preferred, higher emphasis on relocation cost is appropriate. If reducing the number of stations and controlling operating expenses is more important, greater weight should be placed on station cost. The model therefore provides flexibility while maintaining transparency in how different priorities affect the resulting line configurations.

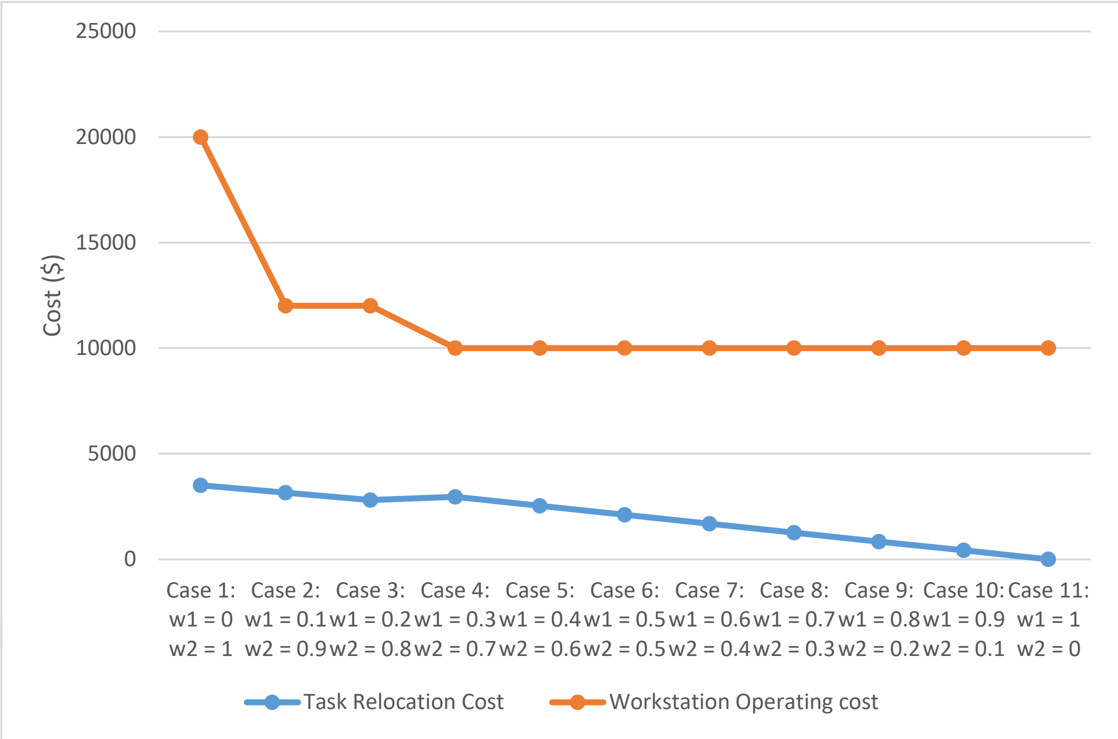

Figure 5.5 Rebalancing cost results for P10-OR

$(CT_1 = 55, CV = 0.25, \alpha = 0.95)$

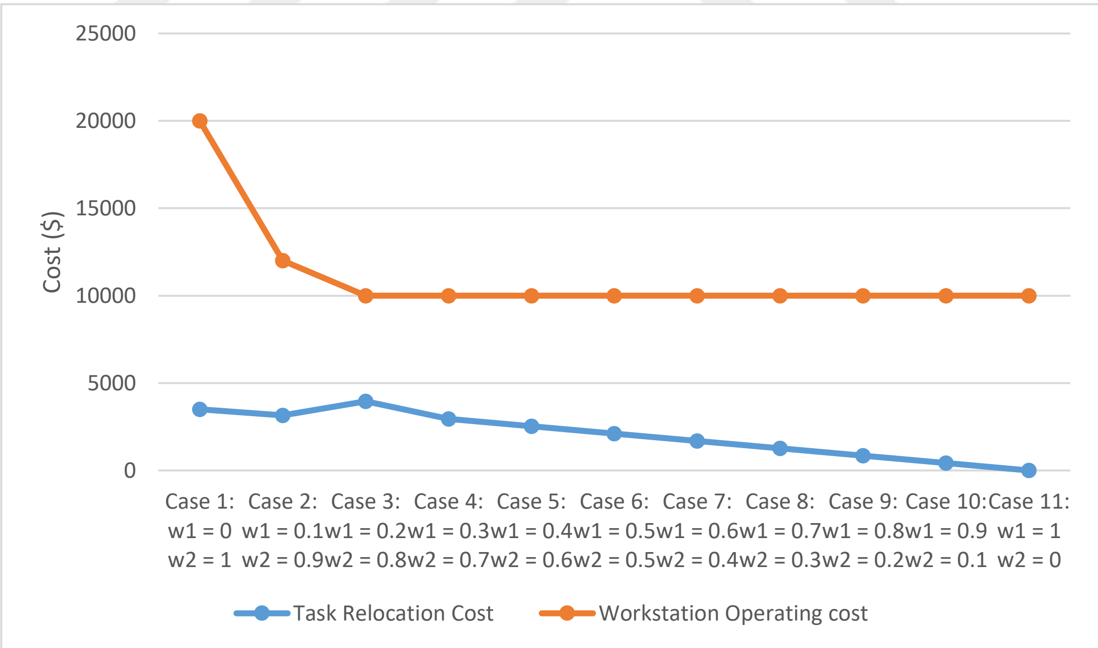

Figure 5.6 Rebalancing cost results for P10-OR

$(CT_1 = 55, CV = 0.25, \alpha = 0.975)$

The results for all instances are represented in the Appendix section. For further information, the full model code, input data, and the experimental results are publicly available at https://github.com/LanaManla/A-Path-Dependent-Multi-Period-Rebalancing-Model-for-Stochastic-U-Shaped-Disassembly-Lines.

To analyze and demonstrate the results obtained for all instances for further understanding of the outcomes, Figures 5.7 and 5.8 illustrate the rebalancing cost trends for all instances across all demand scenarios in low and high variability conditions, respectively.

Figure 5.7 presents the evolution of rebalancing costs across all scenario cases under low variability (CV = 0.1). Starting with the high demand scenario, as expected, the overall cost levels is shown as elevated due to frequent task reallocations and need for station additions driven by tighter cycle time constraints. These conditions force the model to adapt more aggressively, leading to higher cost fluctuations across rebalancing periods. The results show clear differences across instances, where smaller instances such as P10-OR and P22-OR exhibit relatively low and slightly more stabilized costs over time and confidence levels, suggesting greater adaptability. In contrast, larger and more complex instances like P60-OR, P73-OR, and P133-OR show consistently higher rebalancing costs. This reflects the increased burden on the model in maintaining feasibility under uncertainty when fewer operational flexibilities are available.

Furthermore, the impact of the chance-constrained formulation becomes clearer as the required confidence level increases, leading to more conservative solutions. As a result, the model often requires additional stations or incurs increased relocation penalties to maintain the desired level of reliability.

In the low demand scenario in Figure 5.7, it can be noticed that most of the instances follows the same pattern starting with a high cost in the first period and then costs dropping and stabilizing at some point. This behavior reflects the model’s ability to stabilize the line configuration as cycle time increases over time, reducing the need for task relocations or additional stations.

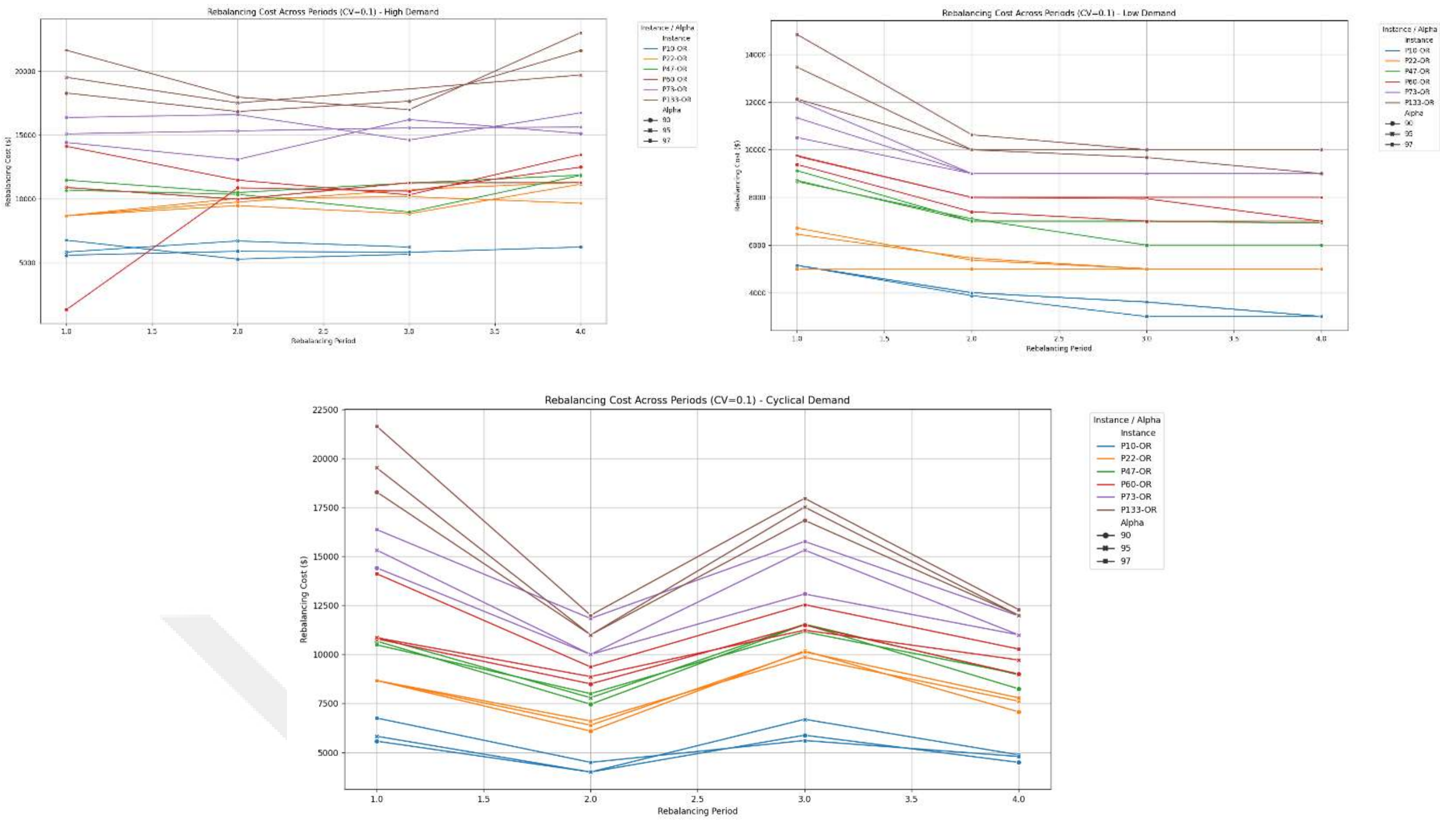

Figure 5.7 Rebalancing cost (RC) across all scenarios for a CV = 0.1

Smaller instances like P10-OR and P22-OR demonstrate sharp initial cost reductions between the first and second periods, followed by minimal changes in subsequent periods, suggesting that smaller systems tends to reach a stable and cost-efficient configuration relatively earlier. Larger instances such as P75-OR and P133-OR also exhibit significant cost reductions. Notably, for several instances (e.g., P73-OR, P60-OR), the rebalancing cost stabilizes completely after the second or third period in most α levels, demonstrating that once an optimal configuration is reached, the model avoids unnecessary reconfigurations. This is a direct result of the path-dependent rebalancing logic, which penalizes excessive task movements and aim to maintain configuration consistency. Furthermore, while higher confidence levels (e.g., α = 97.5%) lead to slightly elevated cost baselines due to the conservative feasibility margins imposed by the chance-constraint formulation, these costs also stabilize over time, highlighting the robustness and reliability of the proposed model even under low uncertainty.

In the cyclical demand scenario, it can be noticed that the cost patterns follow the cyclical fluctuations in cycle time in Figure 5.7, displaying a distinct "V-shape" across all instances and confidence levels. The rebalancing costs starts high in the first period due to a sudden demand increase and then drop in the second period when cycle time loosens (i.e., demand decreases), then peak again in the third period as cycle time tightens due to another increasing of demand. The final period sees a reduction in costs as cycle time relaxes once more. This behavior highlights the model's ability to adapt flexibly to varying demand conditions, responding with cost-efficient line reconfigurations in both the expansion and contraction phases. The cost differences across α levels remain consistent, with higher confidence (such as 97%) incurring slightly higher costs due to stricter chance constraints.

Overall, the results in Figure 5.7 show how the effect of instance size and reliability requirements for different demand scenarios shape the cost dynamics on rebalancing cost behavior, providing meaningful insights onto how the flexibility and uncertainty in the system jointly shape the cost-efficiency in the context of line rebalancing decisions over time.

Figure 5.8 illustrates the rebalancing cost trajectories across periods for all problem instances under a high task time variability (CV = 0.25). When compared to the lower variability case in Figure 5.7, it can be noticed that the rebalancing costs are significantly elevated, and several instances show partial or complete infeasibility, particularly at higher confidence levels (α = 95%, 97.5%) in the high demand scenario.

The absence of feasible solutions in later periods for some instances in the high demand scenario is attributed to the nature of the chance constraint, which imposes tighter probabilistic bounds on station loads, because as task duration variability increases, the uncertainty range around task durations increases, forcing the model to impose stricter safety margins on total station loads. As a result, under tight cycle time limits which is typical of high-demand conditions, the feasible region shrinks considerably, making it increasingly difficult to identify valid task-to-station assignments that satisfy all precedence and probabilistic time constraints simultaneously.

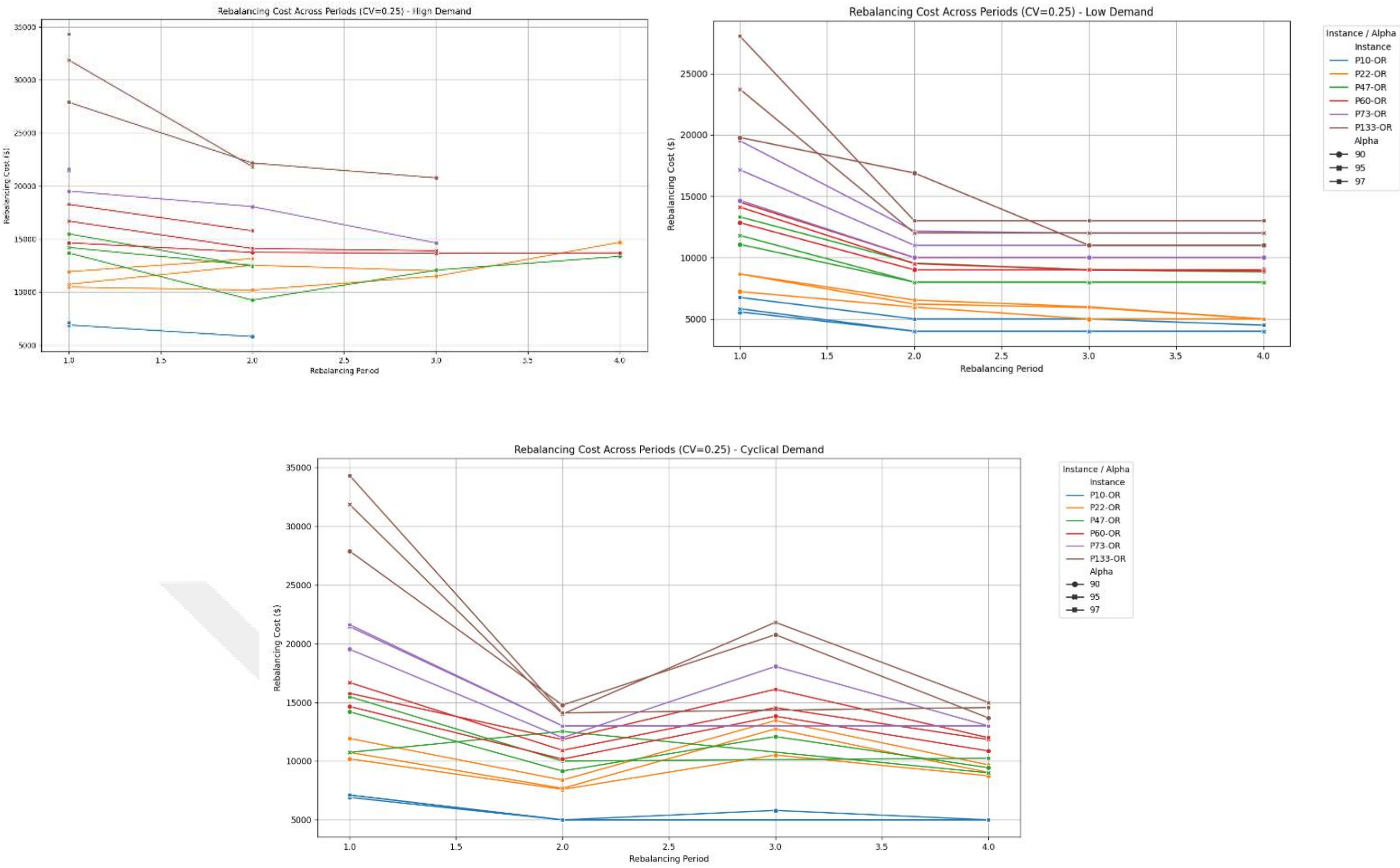

Figure 5.8 Rebalancing cost (RC) across all scenarios for a CV = 0.25

To investigate this situation further, we reformulated the chance-constraint using a Mixed-Integer Second-Order Cone Programming (MI-SOCP) approach following a similar MI-SOCP methodology in Şahin (2022).

In this approach, instead of using a linear approximation for the variance term as expressed in section 4.1, the stochastic component $\sqrt{\sum \sigma_i^2}$ is represented exactly through a conic transformation this time. Specifically, we introduced an auxiliary continuous variable t_m and constrained via a quadratic cone:

$$t_m^2 \geq \sum_{i \in W_m} \sigma_i^2 \, x_{im}$$

Which ensures that:

$$\sqrt{\sum_{i \in W_m} \sigma_i^2 \, x_{im}} \le t_m$$

In this case the chance-constraint then becomes a convex MI-SOCP inequality represented as:

$$\sum_{i \in W_m} \mu_i + z_{1-\alpha}.t_m \le z_m \cdot CT_p$$

After replacing the linear approximation with the exact MI-SOCP representation, the cases the encountered the infeasibility -specifically in the high-demand, CV = 0.25, and high confidence levels cases- were resolved again under the exact same parameter combinations on GAMS using the Gurobi solver. However, the same infeasible cases previously encountered remained infeasible even after changing the linearization method.

This confirms that the infeasibilities are not caused by the linearization method, but by the structure of the parameters themselves. When the required cycle time becomes very short while the variability (CV) and the confidence level are high (e.g., α = 0.95, 0.975), the chance-constraint imposes a safety buffer that simply cannot fit within the available cycle time. Thus, in such cases, no feasible assignment exists because the operating conditions inherently violate probabilistic feasibility and not due to modeling limitations.

In the low demand scenario, the same behavior observed in the lower variability case in Figure 5.7 is exhibited but with higher initial rebalancing costs in the first period and then costs drops and completely stabilizes in later periods. This behavior was especially clear in the large-sized instances. This shows how the path-dependency continue to persist even under high variability with the model's ability to "settle down" and conserve resources when demand is low.

In the cyclical demand scenario, when comparing both variability cases, it can be noticed that the V-shaped pattern is still observed in the CV = 0.25 settings as well, however, with some notable differences. Under CV = 0.1, in Figure 5.7, the rebalancing cost trajectory tends to form a distinct V-shaped pattern across periods, indicating sharp responsiveness to cyclical shifts in cycle time. In contrast, under high variability (CV = 0.25) in Figure 5.8, the same cyclical pattern remains but with a smoother and more flattened profile, particularly in smaller and medium problem instances such as P10-OR, P22-OR, and P47-OR. This reflects the model's conservative behavior in the presence of greater uncertainty, where it opts for less dynamic configurations to satisfy chance constraints. Consequently, cost fluctuations are inhibited, as the system buffers itself against variability by limiting drastic reconfiguration steps.

In addition to evaluating rebalancing cost behavior, computation performance was also evaluated by analyzing the CPU times as illustrated in Figure 5.9 in order to get some insights into how the model scales with increasing instance size and task time variability. As shown in Figure 5.9, it can be noticed that the average CPU times increases nonlinearly as the problem size increase, demonstrating the growing computation complexity associated with larger problem instances.

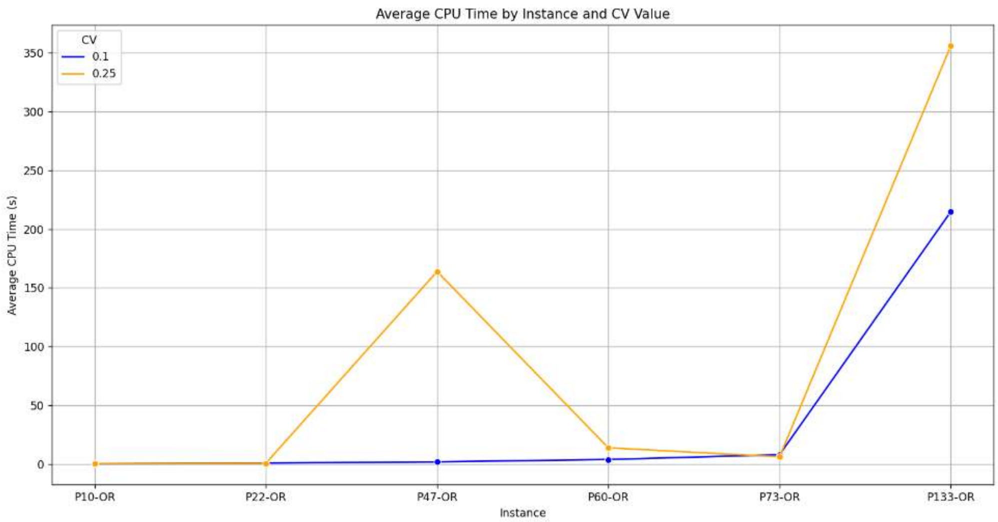

Figure 5.9 Average CPU Time (s) vs problem instances

For smaller instances such as P10-OR and P22-OR, the model exhibits very fast solution times under both low (CV = 0.1) and high (CV = 0.25) variability levels, with average runtimes less than one second, showing that the proposed model is computationally efficient and scalable for small to moderate sized instances. However, in larger instances such as P73-OR and P133-OR, the CPU time increases significantly, particularly under high variability. For example, P133-OR required an average of 356 seconds at CV = 0.25, reflecting the increased computational burden of solving large-scale chance-constrained problems with high uncertainty.

Interestingly, even medium-sized instances can exhibit notable sensitivity to variability. For example, P47-OR showed a dramatic jump in average runtime from 1.7 seconds at CV= 0.1 to over 160 seconds at CV = 0.25, indicating that even medium-sized instances can become computationally intensive under adverse conditions and the interaction between problem size and uncertainty level plays a critical role in determining computational performance.

Overall, the trends observed in Figure 5.9 highlight that while the proposed stochastic, multi-period rebalancing MILP model remains computationally tractable for small and medium instances, solution time increases considerably for large-scale and high-uncertainty scenarios. This behavior is consistent with and observed in the theoretical expectations for mixed-integer stochastic optimization models and highlights the trade-off between model accuracy and computational efficiency in practical applications.

5.3 Comparative Analysis

To further evaluate the effectiveness of the proposed path-dependent multi-period rebalancing framework, a comparative analysis is conducted using the same set of problem instances in Table 5.1, where the same problem instances were resolved independently this time to show a comparison between each rebalancing strategy, illustrating the differences in performance between the proposed approach and the conventional independent rebalancing strategy in terms of the costs saved by each approach, all presented in Table 5.3.

We benchmarked our sequential, path-dependent model against an independent per-period baseline by resolving all of the instances again, but this time independently, under the exact same parameters, where the line is rebalanced from the initial configuration repeatedly in each period whenever a change in demand occurs. In Table 5.3, we computed the average total RC across α levels (independent vs path-dependent) to make the results easier for the eye and accordingly, an average savings per instance were calculated.

The results show that our path-dependent approach consistently outperforms the independent strategy with average savings ranging from 9% to 35% in the high demand scenario where cycle times are progressively reduced. This improvement underscores the value of the model's memory mechanism by keeping information from previous configurations, illustrating how the memory (path-dependency) in the line prevents redundant reallocations and unnecessary station additions under tight cycle times, both of which are common in the independent rebalancing approach under tight cycle time limits.

The cyclical demand scenario similarly showed also strong performance benefits, with savings between 1% and 30%, demonstrating that path-dependency is particularly valuable in dynamic environments with frequent demand fluctuations by responding to fluctuating cycle times, avoiding over-adjustments in expansion and contraction phases, and resulting in smoother and more cost-efficient transitions between rebalancing periods.

Table 5.3 Rebalancing costs of path-dependent vs. independent approach

Scenario	Instance	CV	Avg. Path-Dependent (RC)	Avg. Independent (RC)	Savings (%)
High	P10-OR	0.1	\$19.959	\$22.382,2	11%
		0.25	\$6.676	\$9.413,3	29%
	P22-OR	0.1	\$39.014,6	\$43.125,5	10%
		0.25	\$35.737,5	\$39.422,2	9%
	P47-OR	0.1	\$43.411,8	\$51.494,8	16%
		0.25	\$34.329	\$41.756,5	18%
	P60-OR	0.1	\$42.648,3	\$57.661,2	26%
		0.25	\$44.829,5	\$53.125,8	16%
	P73-OR	0.1	\$61.582,6	\$73.828,5	17%
		0.25	\$31.759,3	\$35.517,5	11%

	P133-OR	0.1	$70.260	$108.101,3	35%
		0.25	$52.932,2	$67.062,6	21%
Low	P10-OR	0.1	$15.511,5	$14.595,6	-6%
		0.25	$18.883,5	$21.158,6	11%
	P22-OR	0.1	$21.329,2	$21.056,5	-1%
		0.25	$25.067,3	$24.432,2	-3%
	P47-OR	0.1	$29.148,2	$28.456	-2%
		0.25	$37.198,5	$42.423,6	12%
	P60-OR	0.1	$32.404	$30.622	-6%
		0.25	$41.972,6	$42.919	2%
	P73-OR	0.1	$38.313,3	$38.313,3	0%
		0.25	$50.164,8	$52.294,8	4%
	P133-OR	0.1	$43.251,8	$42.484,8	-2%
		0.25	$55.226	$72.416,6	24%
Cyclical	P10-OR	0.1	$20.996,6	$23.389,3	10%
		0.25	$18.975,83	$22.383,6	15%
	P22-OR	0.1	$32.574,8	$32.864,5	1%
		0.25	$40.239,5	$41.909,2	4%
	P47-OR	0.1	$38.578,5	$44.166,5	13%
		0.25	$37.631,8	$46.628,3	19%
	P60-OR	0.1	$42.255,6	$48.368	13%
		0.25	$53.082,2	$64.249,3	17%
	P73-OR	0.1	$52.031,6	$58.567,63	11%
		0.25	$52.550,2	$65.121	19%

P133-OR	0.1	$60.693,8	$75.169,8	19%
	0.25	$74.251,67	$106.697,8	30%

The low demand scenario, where cycle times gradually increase, the results were more mixed, with savings ranging from –6% to 24%. This variability can be explained by the fact that, in some instances, the independent strategy managed to reduce the number of stations as cycle times increased, temporarily lowering operating costs in the short term. However, these gains were offset in the long run by relocation penalties, making the path-dependent strategy still advantageous overall, with stabilization of the line proving to be more valuable than incremental station reductions.

To provide a single aggregated measure of improvement, we calculated the weighted average for the overall savings across instances.

The findings showed an average cost reduction of approximately 20% in the high-demand scenario with the path-dependent approach relative to independent rebalancing, reflecting its ability to avoid excessive task relocations under tight cycle time constraints. Similarly, in the cyclical demand scenario, cost savings averaged 17%, demonstrating that path-dependency effectively mitigates unnecessary adjustments in response to demand fluctuations. Even in the low demand scenario, our path-dependent approach still maintained superiority, yielding a 5% cost reduction across all instances, showing that path-dependency saves more in total. This is particularly notable because, in several instances, the independent strategy achieved station reductions (and therefore lower operating costs) as cycle times increased. However, these reductions were accompanied by additional relocations, which offset the potential savings. In contrast, our path-dependent strategy stabilized the line configuration early, avoiding further relocations in later periods and still delivering overall lower costs. These results suggest that long-term stabilization of the line is more beneficial than incremental station reductions, highlighting the practical value of path-dependent rebalancing for cost-efficient and reliable disassembly line management.

Overall, these results highlighted that our sequential, path-dependent model consistently achieved superior cost reduction across all demand scenarios, outperforming the independent rebalancing strategy commonly adopted in the literature.

Based on the results discussed and the observations noticed, it is evident that our model and the framework adopted is tend to be more of a decision-support tool rather than just an optimization tool. Instead of just giving a one-time best solution for a certain moment, it helps plan over time, considering future implications and trade-offs. Our model helps decision-makers to:

1. Evaluate the cost-benefit of rebalancing to see when rebalancing is actually needed and helps avoid overreacting to small demand changes as in rebalancing independently.
2. Plan for different horizons, where managers can test a 1-month vs. 3-month plan and see which is more cost-efficient under uncertainty.
3. Control the risk level, managers can adjust the confidence level (α) to match their tolerance for late task completion.
4. Simulate future conditions and "what-if" scenarios before acting.

Therefore, in practice, the proposed model can be used to help telling decision-makers not just what to do, but also when and whether it's worth doing.

CHAPTER 6
CONCLUSION

The process of eliminating an existing system and building another one from scratch is both costly and time-consuming. Instead, it is more practical to reconfigure the current line to accommodate changing operational requirements. While existing studies have explored rebalancing as a one-time process, these typically assume that the system is re-optimized from the initial configuration repeatedly. In contrast, real-world disassembly systems evolve -previous configurations influence future decisions- and rebalancing is not isolated but rather sequential and path-dependent. This paper develops a novel multi-period, path dependent rebalancing MILP model for U shaped disassembly lines under stochastic task times. Integrating chance constraints to manage task duration uncertainty and accounting for both workstation operating and relocation costs, the proposed model effectively captures realistic rebalancing dynamics driven by fluctuating demand.

The objective of the developed model is to minimize the task relocation and station operating costs that are induced by cycle time alterations in response to changes in demand. To evaluate the model's performance, a comprehensive experimental setup is designed involving multiple demand-driven scenarios, task time uncertainties, and confidence levels. The model was tested and benchmarked on instances from the literature and solved using GAMS-DICOPT solver.

The comparative analysis highlighted the superiority of our sequential, path-dependent approach over independent per-period rebalancing. On average, the proposed model achieved cost savings of approximately 20% under high-demand conditions, 17% under cyclical demand, and 5% under low-demand scenarios. These improvements stem from the ability of the model to stabilize line configurations over time, avoiding unnecessary reallocations and over-adjustments while still adapting flexibly to demand fluctuations.

Additionally, a sensitivity analysis on cost-weight parameters was conducted to assess the model's robustness highlighting a trade-off between relocation cost and station operating cost, where improving one tends to worsen the other. This implied that the choice of weights parameters can be guided directly based on managerial priorities.

The study also showed that infeasible solutions only appear when the cycle time becomes too short while task times are highly variable and the confidence level is very strict. Under these extreme conditions, it is simply impossible to meet the required safety buffer. This was confirmed by testing another linearization method revealing that the infeasibilities are related to the structure of the parameters themselves and not to linearization method limitations.

Overall, the proposed model demonstrates efficacy in dynamically rebalancing disassembly lines under uncertainty, maintaining operational feasibility while minimizing reconfiguration costs. In addition, it functions as a decision-support system telling managers what to do, when and whether it is worth doing, which is essential for effective and reliable operations planning.

Future studies could explore integrating the proposed method with other heuristic techniques and applying it to the re-balancing of mixed-model U-shaped lines. In addition to addressing changes in demand, future research could also consider scenarios involving equipment failures, such as workstation malfunctions or the use of robots. Moreover, different disassembly line configurations like two-sided or parallel lines could be investigated within the context of re-balancing strategies.

REFERENCES

Agrawal, S., & Tiwari, M. K. (2008). A collaborative ant colony algorithm to stochastic mixed-model U-shaped disassembly line balancing and sequencing problem. *International Journal of Production Research, 46*, 1405-1429.

Agpak, K., & Gokcen, H., (2007). A chance-constrained approach to stochastic line balancing problem. *EUROPEAN JOURNAL OF OPERATIONAL RESEARCH* , vol.180, 1098-1115

.Agpak, K. (2010), "An approach to find task sequence for rebalancing of assembly lines", *Assembly Automation, 30 (4)*, 378-387.

Altekin, F. T., & Akkan, C. (2012). Task-failure-driven rebalancing of disassembly lines. *International Journal of Production Research, 50*, 4955-4976.

Altekin, F. T., Kandiller, L., & Ozdemirel, N. E. (2008). Profit-oriented disassembly-line balancing. *International Journal of Production Research, 46*, 2675-2693.

Altemeier, S., Helmdach, M., Koberstein, A. and Dangelmaier, W. (2009), "Reconfiguration of assembly lines under the influence of high product variety in the automotive industry – a decision support system", *International Journal of Production Research, 48 (21)*, 6235-6256.

Avikal, S., Jain, R., & Mishra, P. (2013). A heuristic for U-shaped disassembly line balancing problems. *MIT International Journal of Mechanical Engineering, 3*, 51-56.

Avikal, S., & Mishra, P. (2012). A new U-shaped heuristic for disassembly line balancing problems. *Internaional Journal of Science, 1*, 2277-7261.

Baykasoğlu, A. and Özbakır, L. (2007), "Stochastic U-line balancing using genetic algorithms", *The International Journal of Advanced Manufacturing Technology, 32,* 139-147.

Bagher, M., Zandieh, M. and Farsijani, H. (2011), "Balancing of stochastic U-type assembly lines: an imperialist competitive algorithm", *The International Journal of Advanced Manufacturing Technology, 54,* 271-285.

Corominas, A., Pastor, R. and Plans, J. (2008), "Balancing assembly line with skilled and unskilled workers", *The International Journal of Management Science, 36*, 1126-1132.

Celik, E., Kara, Y. and Atasagun, Y. (2014), "A new approach for re-balancing of U-lines with stochastic task times using ant colony optimization algorithm", *International Journal of Production Research, 52 (24)*, 7262-7275.

Chiang, W.C. and Urban, T.L. (2006), "The stochastic u-line balancing problem: a heuristic procedure", *European Journal of Operational Research, 175 (3)*, 1767-1781.

Çimen, T., Baykasoglu, A. and Akyol, S.D. (2022). A detailed review and analysis of assembly line rebalancing problems. *Assembly Automation, 42,* 742-760.

Ding, L.-P., Feng, Y.-X., Tan, J.-R., & Gao, Y.-C. (2010). A new multi-objective ant colony algorithm for solving the disassembly line balancing problem. *The International Journal of Advanced Manufacturing Technology, 48*, 761-771.

Delice, Y., Kızılkaya Aydoğan, E., & Özcan, U. (2016). Stochastic two-sided U-type assembly line balancing: a genetic algorithm approach. *International Journal of Production Research*, *54*(11), 3429–3451.

Erel, E., Sabuncuoglu, I., & Aksu, B. A. (2001). Balancing of U-type assembly systems using simulated annealing. *International Journal of Production Research, 39*, 3003-3015.

Farahani S., Otieno, W., Barah, M. (2019). Environmentally friendly disposition decisions for end-of-life electrical and electronic products: The case of computer remanufacture. *Journal of Cleaner Production 224*, 25-39.

Fathi, M., Nourmohammadi, A., NG, A. H. C., and Syberfeldt, A. (2019). An Optimization Model for Balancing Assembly Lines With Stochastic Task Times and Zoning Constraints. *IEEE Access, 7.*

Foroughi, A., Gökçen, H. and Tiacci, L. (2016), "The costoriented stochastic assembly line balancing problem: a chance constrained programming approach", *International Journal of Industrial Engineering: Theory, Applications and Practice,23 (6)*, 412-430.

Güngör, A., & Gupta, S. M. (2001). A solution approach to the disassembly line balancing problem in the presence of task failures. *International Journal of Production Research, 39*, 1427-1467.

Güngör, A., & Gupta, S. M. (1999). Disassembly Line Balancing. In *Proceedings of the Annual Meeting of the Northeast Decision Sciences Institute* (pp. 193-195). Newport, RI.

Güngör, A., & Gupta, S. M. (2002). Disassembly line in product recovery. *International Journal of Production Research, 40*, 2569-2589.

Goksoy Kalaycilar, E., Batun, S., & Azizoğlu, M. (2022). A Disassembly Line Balancing Problem with Hazardous Task Failures. *IFAC PapersOnLine*, *55*(10), 458–465.

Gamberini, R., Grassi, A., Rimini, B., 2006. A new multi-objective heuristic algorithm for solving the stochastic assembly line re-balancing problem. *International Journal of Production Research, 102*, 226-243.

Gamberini, R., Gebennini, E., Grassi, A., Regattieri, A., 2009. A multiple single-pass heuristic algorithm solving the stochastic assembly line rebalancing problem. *International Journal of Production Research, 47 (8)*, 2141-2164.

Hu, Y., Liu, C., Zhang, M., Jia, Y., & Xu, Y. (2023). A Novel Simulated Annealing-Based Hyper-Heuristic Algorithm for Stochastic Parallel Disassembly Line Balancing in Smart Remanufacturing. *Sensors, 23*(3), 1652.

Kalayci, C. B., & Gupta, S. M. (2013a). Ant colony optimization for sequence-dependent disassembly line balancing problem. *Journal of Manufacturing Technology Management, 24*, 413-427.

Kalayci, C. B., & Gupta, S. M. (2013b). Artificial bee colony algorithm for solving sequence-dependent disassembly line balancing problem. *Expert Systems with Applications, 40*, 7231-7241.

Kalayci, C. B., & Gupta, S. M. (2013c). A particle swarm optimization algorithm with neighborhood-based mutation for sequence-dependent disassembly line balancing problem. *The International Journal of Advanced Manufacturing Technology, 69*, 197-209.

Koc, A., Sabuncuoglu, I., & Erel, E. (2009). Two exact formulations for disassembly line balancing problems with task precedence diagram construction using an AND/OR graph. *IIE Transactions, 41*, 866-881.

Kalaycilar, E. G., Azizoğlu, M., & Yeralan, S. (2016). A disassembly line balancing problem with fixed number of workstations. *European Journal of Operational Research*, 592–604.

Li, Z., Çil, Z. A., Mete, S., & Kucukkoc, I. (2020). A fast branch, bound and remember algorithm for disassembly line balancing problem. *International Journal of Production Research, 58*, 3220-3234.

Li, Z., Kucukkoc, I., & Zhang, Z. (2019). Iterated local search method and mathematical model for sequence-dependent U-shaped disassembly line balancing problem. *Computers & Industrial Engineering, 137*, 106056.

Li, Z., Kucukkoc, I., Tang, Q., & Zhang, Z. (2021). Models and two-phase bee algorithms for multi-objective U-shaped disassembly line balancing problem. *Optimization and Engineering, 24*, 591-622.

McGovern, S.M., Gupta, S.M., 2007. A balancing method and genetic algorithm for disassembly line balancing. *European Journal of Operational Research, 179 (3)*, 692-708.

Makssoud, F., Battaïa, O. and Dolgui, A. (2014), "An exact optimization approach for a transfer line reconfiguration problem", *The International Journal of Advanced Manufacturing Technology, 72*, 717-727.

Makssoud, F., Battaïa, O. and Dolgui, D. (2015), "Rebalancing problem for assembly lines: new mathematical model and exact solution method", *Assembly Automation, 35*, 16-21.

Mete, S., Çil, Z. A., Ağpak, K., Özceylan, E., & Dolgui, A. (2016). A solution approach based on beam search algorithm for disassembly line balancing problem. *Journal of Manufacturing Systems, 41*, 188-200.

Mete, S., Çil, Z.A., Özceylan, E., Ağpak, K., (2016b). Resource constrained disassembly line balancing problem. IFAC-PapersOnLine 49 (12), 921-925.

Mete, S., Cil, Z.A., Ozceylan, E., Agpak, K., Battaia, O., 2018. An optimization support for the design of hybrid production lines including assembly and disassembly tasks. *International Journal of Production Research.*

Mete, S., Çil, Z.A., Celik, E. and Ozceylan, E. (2019), "Supply-driven rebalancing of disassembly lines: a novel mathematical model approach", *Journal of Cleaner Production, 213,* 1157-1164.

Miltenburg, G. J., & Wijngaard, J. (1994). The U-Line Line Balancing Problem. *Management Science, 40*, 1378-1388.

Oliveria, F.S., Vittori, K., Rusell, R.M.O. and Travassos, X.L. (2012), “Mixed assembly line re-balancing: a binary integer approach applied to real world problems in the automotive industry”, *International Journal of Automotive Technology, 13*, 933-940.

Özcan, U. (2009). Balancing stochastic two-sided assembly lines: A chance-constrained, piecewise-linear, mixed integer program and a simulated annealing algorithm. *European Journal of Operational Research, 205.* 81-97.

Özceylan, E., Kalayci, C. B., Güngör, A., & Gupta, S. M. (2018). Disassembly line balancing problem: a review of the state of the art and future directions. *International Journal of Production Research, 57*, 4805-4827.

Paksoy, T., Güngör, A., Özceylan, E., & Hancilar, A. (2013). Mixed model disassembly line balancing problem with fuzzy goals. *International Journal of Production Research, 51*, 6082-6096.

Ren, Y., Yu, D., Zhang, C., Tian, G., Meng, L., & Zhou, X. (2017). An improved gravitational search algorithm for profit-oriented partial disassembly line balancing problem. *International Journal of Production Research, 55*, 7302-7316.

Silverman, F.N. and Carter, J.C. (1986), “A cost-based methodology for stochastic line balancing with intermittent line stoppages”, *Management Science, 32 (4),* 455-463.

Scholl, A., & Klein, R. (1999). ULINO: Optimally balancing U-shaped JIT assembly lines. *International Journal of Production Research, 37*, 721-736.

Sancı, E. and Azizoğlu, M. (2017), “Re-balancing the assembly lines: exact solution approaches”, *International Journal of Production Research, 55 (20)*, 5991-6010.

Serin, F., Mete, S., and Çelik, E. (2019), An efficient algorithm for U-type assembly line re-balancing problem with stochastic task times. *Assembly Automation, 39 (4)*, 581-595.

Şahin, M. C. (2022). *Stochastic Assembly Line Balancing Problems Involving Robots and Reliability Restriction* (Master's thesis, Middle East Technical University (Turkey)).

Wang, K., Ma, X., Li, Y., Luo, Y., Li, Y., and Gao, L. (2025). An adaptive genetic algorithm based on Q-learning for energy-efficient e-waste disassembly line balancing and rebalancing considering task failures. *Journal of Manufacturing Systems, 80,* 1-19.

Xiao, S., Wang, Y., Yu, H., & Nie, S. (2017). An Entropy-Based Adaptive Hybrid Particle Swarm Optimization for Disassembly Line Balancing Problems. *Entropy, 19*, 596.

Xu Z, Han Y. (2023). Two-sided disassembly line balancing problem with rest time of works: a constraint programming model and an improved NSGA II algorithm. *Expert Systems with Applications, 239.*

Yang, C., Gao, J., Sun, L., 2013. A multi-objective genetic algorithm for mixed-model assembly line rebalancing. *Computers & Industrial Engineering*, 65, 109-116.

Yılmaz, Ö.F., Yazıcı, B. (2022). Tactical level strategies for multi-objective disassembly line balancing problem with multi-manned stations: an optimization model and solution approaches. *Annals of Operations Research 319,* 1793–1843.

Zha, J., Yu, J.J., 2014. A hybrid ant colony algorithm for U-line balancing and rebalancing in just-in-time production environment. *Journal of Manufacturing Systems*, 33, 93e102.

Zhang, Z., Wang, K., Zhu, L., & Wang, Y. (2017). A Pareto improved artificial fish swarm algorithm for solving a multi-objective fuzzy disassembly line balancing problem. *Expert Systems with Applications, 86*, 165-176.

Zhang, Y., Hu, X. and Wu, C. (2018), “A modified multiobjective genetic algorithm for two-sided assembly line rebalancing problem of a shovel loader”, *International Journal of Production Research, 56(9)*, 3043-3063.

APPENDIX A

Table A.1 Scenario 1: High Demand (For all instances)

Instance	CV	1- α	Period_p	CT_{p-1}	CT_p	RC	#NS	CPU (s)
P10-OR	0.1	90	1	60	55	$5574.50	4	0.141
			2	55	50	$5879.50	5	0.141
			3	50	45	$5804	5	0.125
			4	45	41	$6215	5	0.125
		95	1	60	55	$5826	4	0.390
			2	55	50	$6690	5	0.109
			3	50	45	$6215	5	0.110
			4	45	41	-	-	0.109
		97.5	1	60	55	$6753	5	0.406
			2	55	50	$5266.50	5	0.110
			3	50	45	$5653.50	5	0.109
			4	45	41	-	-	0.110
	0.25	90	1	60	55	$6904	5	0.125
			2	55	50	$5804	5	0.141
			3	50	45	-	-	0.094
			4	45	41	-	-	0.110
		95	1	60	55	$7112	5	0.125
			2	55	50	-	-	0.266
			3	50	45	-	-	0.078
			4	45	41	-	-	0.078
		97.5	1	60	55	$7112	5	0.125
			2	55	50	-	-	0.063
			3	50	45	-	-	0.078

			4	45	41	-	-	0.093
P22-OR	0.1	90	1	50	46	$8667.50	7	2.250
			2	46	40	$9463.50	8	1.094
			3	40	37	$8828.50	8	0.188
			4	37	34	$11145	9	0.531
		95	1	50	46	$8667.50	7	2.562
			2	46	40	$10031	8	0.594
			3	40	37	$10163.50	9	0.375
			4	37	34	$9655	9	0.219
		97.5	1	50	46	$8667.50	7	0.844
			2	46	40	$9743	8	0.469
			3	40	37	$10706.50	9	0.875
			4	37	34	11305.50	10	0.469
	0.25	90	1	50	46	$10473.50	8	1.265
			2	46	40	$10192	9	0.282
			3	40	37	$11497	10	0.312
			4	37	34	$14697	10	1.422
		95	1	50	46	$10741.50	8	0.328
			2	46	40	$12528.50	10	1.344
			3	40	37	$12005.50	10	0.250
			4	37	34	-	-	0.172
		97.5	1	50	46	$11926.50	9	1.484
			2	46	40	$13151	10	0.875
			3	40	37	-	-	0.718
			4	37	34	-	-	0.609
P47-OR	0.1	90	1	81	77	$10681	8	6.015
			2	77	74	$10352.50	8	1.766
			3	74	69	$8957	8	0.785

			4	69	65	$11836	9	1.828
		95	1	81	77	$10884.50	8	4.484
			2	77	74	$9963.50	8	0.813
			3	74	69	$11256	9	2.032
			4	69	65	$11261.50	9	1.375
		97.5	1	81	77	$11466	8	3.953
			2	77	74	$10488.50	8	3.750
			3	74	69	$11231.50	9	0.844
			4	69	65	11857.50	10	1.500
	0.25	90	1	81	77	$13679.50	9	5.843
			2	77	74	$9247	9	0.390
			3	74	69	$12071	10	1.485
			4	69	65	$13363	10	9.313
		95	1	81	77	$14202.50	9	5.188
			2	77	74	$12523	10	0.953
			3	74	69	-	-	0.625
			4	69	65	-	-	0.203
		97.5	1	81	77	$15487.50	10	4.500
			2	77	74	$12413.50	10	2.328
			3	74	69	-	-	0.203
			4	69	65	-	-	0.203
P60-OR	0.1	90	1	79	74	$1298	9	7.992
			2	74	70	$10853.50	10	1.422
			3	70	67	$10600	10	0.726
			4	67	64	$12478.50	11	3.248
		95	1	79	74	$10884.50	9	4.484
			2	74	70	$9963.50	8	0.813
			3	70	67	$11256	9	2.032

			4	67	64	$11261.50	9	1.375
		97.5	1	79	74	$14118.50	10	7.263
			2	74	70	$11464	10	1.079
			3	70	67	$10306.50	10	0.684
			4	67	64	$13460.50	11	5.314
	0.25	90	1	79	74	$14652	10	4.228
			2	74	70	$13748.50	11	6.995
			3	70	67	$13663.50	12	8.861
			4	67	64	$13696	12	1.791
		95	1	79	74	$16689.50	11	7.397
			2	74	70	$14110.50	12	1.550
			3	70	67	$13894	12	2.107
			4	67	64	-	-	0.365
		97.5	1	79	74	$18263.50	12	4.043
			2	74	70	$15771	12	137.964
			3	70	67	-	-	0.360
			4	67	64	-	-	0.500
P73-OR	0.1	90	1	97	94	$14416.50	10	7.549
			2	94	87	$13084	11	6.102
			3	87	82	$16210	12	46.804
			4	82	77	$15117.50	12	2.636
		95	1	97	94	$15096	10	39.113
			2	94	87	$15327	11	4.659
			3	87	82	$15554.50	12	3.366
			4	82	77	$15618.50	13	0.895
		97.5	1	97	94	$16374	11	40.621
			2	94	87	$16601	12	26.271
			3	87	82	$14608.50	12	1.241

			4	82	77	$16740.50	13	2.065
	0.25	90	1	97	94	$19524	12	5.285
			2	94	87	$18058.50	13	9.030
			3	87	82	$14627.50	13	1.122
			4	82	77	-	-	0.378
		95	1	97	94	$21450	13	47.106
			2	94	87	-	-	1.302
			3	87	82	-	-	0.378
			4	82	77	-	-	0.333
		97.5	1	97	94	$21618	13	10.046
			2	94	87	-	-	0.352
			3	87	82	-	-	0.356
			4	82	77	-	-	0.293
P133-OR	0.1	90	1	165	155	$18292.50	11	50.759
			2	155	143	$16843	12	47.415
			3	143	136	$17652	13	51.172
			4	136	122	$21614.50	14	77.418
		95	1	165	155	$19525.50	11	795.774
			2	155	143	$17516.50	12	39.806
			3	143	136	$18323	13	3680.33
			4	136	122	$19709.50	14	137.025
		97.5	1	165	155	$21647.50	12	581.800
			2	155	143	$17968	13	30.033
			3	143	136	$16989.50	13	4.426
			4	136	122	$23021.50	15	32.473
	0.25	90	1	165	155	$27883.50	13	67.693
			2	155	143	$22160.50	14	47.743
			3	143	136	$20762	15	45.140
			4	136	122	-	-	0.864

95	1	165	155	$31851.50	14	2390.593
	2	155	143	$21819	15	1988.458
	3	143	136	-	-	33.337
	4	136	122	-	-	0.890
97.5	1	165	155	$34320	14	335.672
	2	155	143	-	-	1.095
	3	143	136	-	-	1.115
	4	136	122	-	-	0.985

*Values in **bold** indicates no task relocation. Only workstation operating costs incurred.*

Table A.2 Scenario 2: Low Demand (For all instances)

Instance	CV	1- α	Period_p	CT_{p-1}	CT_p	RC	#NS	CPU (s)
P10-OR	0.1	90	1	60	65	$5146	4	0.125
			2	65	71	$3879.50	3	0.109
			3	71	77	**$3000**	3	0.094
			4	77	83	**$3000**	3	0.094
		95						
			1	60	65	$5146	4	0.125
			2	65	71	**$4000**	4	0.125
			3	71	77	$3608.50	3	0.094
			4	77	83	**$3000**	3	0.109
		97.5						
			1	60	65	$5146	4	0.156
			2	65	71	**$4000**	4	0.109
			3	71	77	$3608.50	3	0.140
			4	77	83	**$3000**	3	0.109
	0.25	90	1	60	65	$5574.50	4	0.438
			2	65	71	**$4000**	4	0.109
			3	71	77	**$4000**	4	0.141
			4	77	83	**$4000**	4	0.125
		95	1	60	65	$5830	4	0.125
			2	65	71	**$4000**	4	0.125
			3	71	77	**$4000**	4	0.125
			4	77	83	**$4000**	4	0.109
		97.5	1	60	65	$6753.50	5	0.141
			2	65	71	**$5000**	5	0.125
			3	71	77	**$5000**	5	0.140
			4	77	83	$4492.50	4	0.125
P22-OR	0.1	90	1	50	58	**$5000**	5	0.141
			2	58	69	**$5000**	5	0.156
			3	69	80	**$5000**	5	0.172
			4	80	91	**$5000**	5	0.172

		95	1	50	58	$6453	6	1.235
			2	58	69	$5453	5	0.234
			3	69	80	**$5000**	5	0.250
			4	80	91	**$5000**	5	0.250
		97.5	1	50	58	$6716.50	6	0.641
			2	58	69	$5365	5	0.234
			3	69	80	**$5000**	5	0.235
			4	80	91	**$5000**	5	0.250
	0.25	90	1	50	58	$7230.50	6	0.281
			2	58	69	$5967	5	0.250
			3	69	80	**$5000**	5	0.203
			4	80	91	**$5000**	5	0.188
		95	1	50	58	$8667.50	7	0.266
			2	58	69	$6212.50	6	0.266
			3	69	80	$5932.50	5	0.234
			4	80	91	**$5000**	5	0.250
		97.5	1	50	58	$8667.50	7	1.079
			2	58	69	$6538.50	6	0.328
			3	69	80	$5986	5	0.500
			4	80	91	**$5000**	5	0.203
P47-OR	0.1	90	1	81	87	$8667.50	7	1.079
			2	87	94	$7098.50	6	0.406
			3	94	98	**$6000**	6	0.250
			4	98	105	**$6000**	6	0.234
		95	1	81	87	$8709	7	1.281
			2	87	94	**$7000**	7	0.500
			3	94	98	**$7000**	7	0.297
			4	98	105	$6921.50	6	0.266

		97.5	1	81	87	$9126.50	7	0.985
			2	87	94	**$7000**	7	0.360
			3	94	98	**$7000**	7	0.375
			4	98	105	$6921.50	6	0.390
	0.25	90	1	81	87	$11081	8	6.875
			2	87	94	**$8000**	8	0.515
			3	94	98	**$8000**	8	0.282
			4	98	105	**$8000**	8	0.235
		95	1	81	87	$11809	8	1.484
			2	87	94	**$8000**	8	0.250
			3	94	98	**$8000**	8	0.266
			4	98	105	**$8000**	8	0.281
		97.5	1	81	87	$13319	9	5.907
			2	87	94	$9552	9	0.391
			3	94	98	**$9000**	9	0.360
			4	98	105	$8834.50	8	0.266
P60-OR	0.1	90	1	79	87	$9384.50	8	8.386
			2	87	97	$7399	7	3.091
			3	97	104	**$7000**	7	0.355
			4	104	115	**$7000**	7	0.346
		95	1	79	87	$9727	8	10.410
			2	87	97	$8000	8	0.546
			3	97	104	$7947	7	0.347
			4	104	115	**$7000**	7	0.361
		97.5	1	79	87	$9754.50	8	14.463
			2	87	97	**$8000**	8	0.581
			3	97	104	**$8000**	8	0.595
			4	104	115	**$8000**	8	0.595
	0.25	90	1	79	87	$12848	9	13.107

			2	87	97	**$9000**	9	0.417
			3	97	104	**$9000**	9	0.409
			4	104	115	**$9000**	9	0.399
		95	1	79	87	$14118.50	10	134.878
			2	87	97	$9507.50	9	0.603
			3	97	104	**$9000**	9	0.466
			4	104	115	$8927.50	8	0.349
		97.5	1	79	87	$14516.50	10	7.758
			2	87	97	**$10000**	10	0.436
			3	97	104	**$10000**	10	0.903
			4	104	115	**$10000**	10	0.850
P73-OR	0.1	90	1	97	107	$10515	9	0.912
			2	107	120	**$9000**	9	0.487
			3	120	128	**$9000**	9	0.500
			4	128	135	**$9000**	9	0.520
		95	1	97	107	$11344	9	0.875
			2	107	120	**$9000**	9	0.833
			3	120	128	**$9000**	9	0.748
			4	128	135	**$9000**	9	0.775
		97.5	1	97	107	$12081	9	3.329
			2	107	120	**$9000**	9	0.435
			3	120	128	**$9000**	9	0.504
			4	128	135	**$9000**	9	0.467
	0.25	90	1	97	107	$14665	10	4.056
			2	107	120	**$10000**	10	0.938
			3	120	128	**$10000**	10	0.453
			4	128	135	**$10000**	10	0.471
		95	1	97	107	$17155	11	42.151
			2	107	120	**$11000**	11	0.524

			3	120	128	**$11000**	11	0.453
			4	128	135	**$11000**	11	0.471
		97.5	1	97	107	$19524	12	17.462
			2	107	120	$12150.50	12	1.441
			3	120	128	**$12000**	12	0.476
			4	128	135	**$12000**	12	0.720
P133-OR	0.1	90	1	165	175	$12133.50	10	571.469
			2	175	187	**$10000**	10	01.442
			3	187	200	$9679.50	9	1.218
			4	200	223	**$9000**	9	1.090
		95	1	165	175	$13470	10	33.685
			2	175	187	**$10000**	10	1.583
			3	187	200	**$10000**	10	1.407
			4	200	223	**$10000**	10	1.506
		97.5	1	165	175	$14842	10	21.822
			2	175	187	$10630.50	10	1.183
			3	187	200	**$10000**	10	0.974
			4	200	223	**$10000**	10	0.976
	0.25	90	1	165	175	$19786	11	3605.48
			2	175	187	$16891	11	48.729
			3	187	200	**$11000**	11	1.064
			4	200	223	**$11000**	11	1.076
		95	1	165	175	$23731	12	123.842
			2	175	187	**$12000**	12	1.186
			3	187	200	**$12000**	12	1.989
			4	200	223	**$12000**	12	1.210
		97.5	1	165	175	$28056	13	163.592
			2	175	187	**$13000**	13	1.768
			3	187	200	**$13000**	13	1.756

	4	200	223	**$13000**	13	1.811

*Values in **bold** indicates no task relocation. Only workstation operating costs incurred.*

Table A.3 Scenario 3: Fluctuated (Cyclical) Demand (For all instances)

Instance	CV	1- α	Period_p	CT_{p-1}	CT_p	RC	#NS	CPU (s)
P10-OR	0.1	90	1	60	55	$5574.50	4	0.141
			2	55	65	**$4000**	4	0.094
			3	65	50	$5879.50	5	0.125
			4	50	60	$4492.50	4	0.109
		95						
			1	60	55	$5826	4	0.390
			2	55	65	**$4000**	4	0.125
			3	65	50	$6690	5	0.125
			4	50	60	$4879.50	4	0.141
		97.5						
			1	60	55	$6753.50	5	0.406
			2	55	65	$4492.50	4	0.125
			3	65	50	$5608.50	5	0.140
			4	50	60	$4793.50	4	0.109
	0.25	90	1	60	55	$6904	5	0.125
			2	55	65	$4995.50	4	0.125
			3	65	50	$5804	5	0.125
			4	50	60	**$5000**	5	0.141
		95	1	60	55	$7112	5	0.125
			2	55	65	**$5000**	5	0.141
			3	65	50	-	-	0.078
			4	50	60	**$5000**	5	0.141
		97.5	1	60	55	$7112	5	0.125
			2	55	65	**$5000**	5	0.093
			3	65	50	**-**	-	0.063
			4	50	60	**$5000**	5	0.125
P22-OR	0.1	90	1	50	46	$8667.50	7	2.250
			2	46	58	$6087.50	5	0.187
			3	58	40	$10182	8	2.250
			4	40	50	$7071.50	6	0.218

		95	1	50	46	$8667.50	7	2.562
			2	46	58	$6602	6	0.328
			3	58	40	$9854	8	0.516
			4	40	50	$7616	6	0.297
		97.5	1	50	46	$8667.50	7	0.844
			2	46	58	$6389.50	6	0.266
			3	58	40	$10132.50	8	0.547
			4	40	50	$7787	7	0.172
	0.25	90	1	50	46	$10192	9	0.282
			2	46	58	$7594	7	0.235
			3	58	40	$10522.50	9	0.234
			4	40	50	$8754	7	0.266
		95	1	50	46	$10741.50	8	0.328
			2	46	58	$7683.50	7	0.250
			3	58	40	$12741	10	1.031
			4	40	50	$9039.50	8	0.266
		97.5	1	50	46	$11926.50	9	1.484
			2	46	58	$8389.50	8	0.375
			3	58	40	$13455	10	0.829
			4	40	50	$9679.50	9	0.360
P47-OR	0.1	90	1	81	77	$10681	8	6.015
			2	77	87	$7458	7	0.297
			3	87	69	$11528	8	5.406
			4	69	81	$8247	8	0.375
		95	1	81	77	$10884.50	8	4.484
			2	77	87	$7790	7	0.390
			3	87	69	$11546.50	9	3.063
			4	69	81	$8958.50	8	0.313

		97.5	1	81	77	$10488.50	8	3.750
			2	77	87	**$8000**	8	0.360
			3	87	69	$11153.50	9	1.718
			4	69	81	**$9000**	9	0.813
	0.25	90	1	81	77	$14202.50	9	5.188
			2	77	87	$9157	9	0.250
			3	87	69	$12089	10	0.937
			4	69	81	$9442.50	9	0.266
		95	1	81	77	$10741.50	8	0.328
			2	77	87	$12528.50	10	1.344
			3	87	69	-	-	0.719
			4	69	81	**$9000**	9	0.266
		97.5	1	81	77	$15487.50	10	4.500
			2	77	87	**$10000**	10	0.234
			3	87	69	-	-	0.187
			4	69	81	$10247	10	0.281
P60-OR	0.1	90	1	79	74	$10795.50	9	4.270
			2	74	87	$8498	8	0.380
			3	87	70	$11498.50	9	5.670
			4	70	79	**$9000**	9	0.641
		95	1	79	74	$10853.50	10	1.422
			2	74	87	$8869.50	8	0.396
			3	87	70	$11237.50	10	3.737
			4	70	79	$9717.50	9	0.500
		97.5	1	79	74	$14118.50	10	7.263
			2	74	87	$9363	8	0.656
			3	87	70	$12540	10	33.267
			4	70	79	$10275.50	9	0.691
	0.25	90	1	79	74	$14652	10	4.228

			2	74	87	$10174	9	0.632
			3	87	70	$13821	11	4.101
			4	70	79	$10869	10	0.987
		95	1	79	74	$16689.50	11	134.878
			2	74	87	$10922.50	10	0.603
			3	87	70	$14551.50	12	0.466
			4	70	79	$11841	11	0.349
		97.5	1	79	74	$15771	12	7.758
			2	74	87	$11838	11	0.436
			3	87	70	$16117	12	0.903
			4	70	79	$12000	12	0.850
P73-OR	0.1	90	1	97	94	$14416.50	10	7.549
			2	94	107	**$10000**	10	0.494
			3	107	87	$13084	11	2.566
			4	87	97	**$11000**	11	0.552
		95	1	97	94	$15327	10	4.659
			2	94	107	**$10000**	10	0.793
			3	107	87	$15327	11	17.174
			4	87	97	**$11000**	11	0.817
		97.5	1	97	94	$16374	11	40.621
			2	94	107	$11834	11	0.476
			3	107	87	$15766.50	12	13.142
			4	87	97	$11966	11	0.560
	0.25	90	1	97	94	$19524	12	5.285
			2	94	107	**$12000**	12	0.521
			3	107	87	$18058.50	13	3.966
			4	87	97	**$13000**	13	0.487
		95	1	97	94	$21450	13	47.106
			2	94	107	**$13000**	13	0.541

			3	107	87	-	-	1.482
			4	87	97	**$13000**	13	0.601
		97.5	1	97	94	$21618	13	10.046
			2	94	107	**$13000**	13	0.603
			3	107	87	-	-	0.376
			4	87	97	**$13000**	13	0.447
P133-OR	0.1	90	1	165	155	$18292.50	11	50.759
			2	155	175	**$11000**	11	1.142
			3	175	143	$16843	12	47.110
			4	143	165	**$12000**	12	1.348
		95	1	165	155	$19525.50	11	795.774
			2	155	175	**$11000**	11	1.678
			3	175	143	$17516.50	12	52.758
			4	143	165	**$12000**	12	1.686
		97.5	1	165	155	$21647.50	12	581.800
			2	155	175	**$12000**	12	1.419
			3	175	143	$17968	13	28.928
			4	143	165	$12288.50	12	1.100
	0.25	90	1	165	155	$27883.50	13	67.693
			2	155	175	$14769	13	1.390
			3	175	143	$20763.50	14	36.280
			4	143	165	$13679.50	13	2.963
		95	1	165	155	$31851.50	14	2390.593
			2	155	175	**$14000**	14	1.024
			3	175	143	$21819	15	9.692
			4	143	165	**$15000**	15	1.330
		97.5	1	165	155	$34320	14	335.672
			2	155	175	$14105.50	14	1.129
			3	175	143	-	-	1.103

4	143	165	$14563.50	14	1.292

*Values in **bold** indicates no task relocation. Only workstation operating costs incurred.*

CURRICULUM VITAE

LANA MANLA ALI

EDUCATION

Degree	Department	University	Years
MSc	Industrial Engineering	Gaziantep University	2023-2025
BSc	Industrial Engineering	Gaziantep University	2019-2023

PUBLICATIONS

Manla Ali, L., Khanji, O., & ÖZCEYLAN, E. (2023, March). Location-Allocation Optimization of Wi-Fi Access Points at Gaziantep University Campus. In *13th Annual International Conference on Industrial Engineering and Operations Management*, https://doi.org/10.46254/AN13.20230576.

Eligüzel, N. & **Ali, L. M.** (2022). Analyzing of Cyber-Security Concepts on Twitter. *European Journal of Scienceand Technology,* (34), 541-545.

Manla Ali, L., Özceylan, E., & Mete, S. (2025). **S**equential rebalancing framework for stochastic U-shaped disassembly lines. In *Proceedings of the 6th International Conference of Materials and Engineering Technology (TICMET'25)* (pp. 439–446). 6–9 October 2025.

PROFESSIONAL EXPERIENCE

Durkar Carpet - Project Development and Management Intern; Gaziantep, Türkiye
(Mar 2023 – June 2023)

- Contributed to the development of projects focused on continuous improvement and lean production principles. I maintained detailed reports of project activities, analyzed data to identify trends and areas for improvement, and provided actionable solutions based on my analysis to enhance project outcomes.

Durkar Carpet - Customer Representative; Gaziantep, Türkiye

(Aug 2023 – Dec 2023)

- Was responsible for all sales activities in the American region, from new customer recruitment to the closing phase. I worked closely with sales and support teams to ensure high customer satisfaction and profitability.

SKILLS

Languages: Arabic, English, Turkish

Technical: Reporting, Strategic and social sales, Data Analysis, Microsoft Office, Lingo program, Gams program, Arena simulation program, Python Program